Origin of the Setouchi Volcanic Rocks in SW Japan Arc: Constraints from Pb-Nd-Sr Isotope Geochemistry

Hajime Shimoda

1996

PREFACE

The chemical evolution of the Earth is one of the most essential problems of geochemistry. The subduction zone is the major site where the chemical differentiation of the Earth has occurred. Principal differentiation processes occurring in subduction zones are dehydration and/or partial melting of the subducted lithosphere. Through these processes, the released aqueous fluid/melt metasomatize the overlying mantle wedge and induce arc magmatism. Further, the subduction zone would be the region where the continental materials are recycled into the Earth's interior. This recycling should have significant effect on the chemical evolution of the Earth's mantle, and would be responsible for causing the chemical heterogeneity within the deep mantle reservoir documented in oceanic island basalts. Therefore, evaluating of the elemental inventory in the downgoing slab based on geochemistry of subduction related lavas provides a key to understanding of the chemical evolution of the Earth.

The radiogenic isotopes, such as Pb, Nd, Sr, Be, *etc.*, provide strong constraints for better understanding of the geochemical consequence of subduction zone magmatism, because these isotopic ratios are invariant during processes both of melting and differentiation which drastically change concentrations of elements. Moreover, the radiogenic isotopic ratios reflect the time integrated parent and daughter nuclide ratios, and are not only the basis of the absolute age determinations but also the tags of the distinctive geochemical reservoirs. In these points of view, isotopic data for arc lavas have contributed significantly to understanding of the genesis of subduction

zone magmas. Among these radiogenic isotopes, Pb isotopic compositions are most powerful tracers for evaluating the recycling of continental crustal material during subduction processes, because continental crust-derived sediments have both Pb-isotope ratios and concentrations quite distinct from mantle rocks.

In this thesis, I reestablish analytical procedures for determination of Pb isotopic compositions, and apply this method to the Setouchi volcanic rocks from the SW Japan arc in order to examine the genesis of these magmas. I also analyzed Nd and Sr isotopic compositions along with major and trace elements compositions for these rocks. These geochemical data together with the previous petrological data enable to provide constraints on the recycling process of crustal materials and the nature of slab-derived subduction component. Further, based on the temporal/spatial variations of Pb isotopic compositions of the Setouchi volcanic rocks, I will discuss the geochemical evolution of the sub-Setouchi mantle wedge during a mega-tectonic event of the opening of the Japan Sea.

Contents

Abstract

In order to clarify the role of subducted sediments in determining the geochemical characteristics of subduction-related magmas and to evaluate the effect of the Japan Sea opening on the geochemical evolution of the mantle wedge, Pb, Sr and Nd isotope studies, along with major and trace element analyses have been carried out for Miocene volcanic rocks from the Setouchi volcanic belt, SW Japan. Pb isotopic compositions of the Setouchi volcanic rocks lie between those of the Japan Sea floor basalts and local sediments with much higher values than the NHRL (Northern Hemisphere Reference Line). Nd-Sr isotopic compositions, on the other hand, fall within the mantle array. Among those samples, high-magnesian andesites (HMAs) have distinctively higher Pb, Sr and lower Nd isotopic compositions than basalts. Trace element compositions of HMAs also show systematically higher Pb, K and Rb concentrations than basalts. These geochemical features may be best explained by the different amounts of added slab-derived subduction component (SDSC). Further, the HFSE (High Field Strength Elements) systematics, including higher Nb/TiO_2 and Zr/TiO_2 ratios of HMAs than those of basalts, suggest that the SDSC is not an aqueous fluid but a partial melt. The major component of SDSC would be derived mainly from subducted terrigenous sediments; however, the minor contribution of the altered MORB crust-derived component is indispensable to explain both isotopic and chemical compositions. The Pb isotopic compositions clearly exhibit secular variation; they had changed from

enriched to relatively depleted with decreasing ages. A plausible interpretation of this isotopic compositional change may be due to the replacement of the original mantle wedge with an enriched geochemical signatures by the laterally injected asthenospheric materials with depleted geochemical signatures which may relate to the south-ward migration of the SW Japan arc sliver and the Japan Sea opening.

Introduction

The subduction zone, where the oceanic crust descends into the mantle, is one of the major sites causing the chemical differentiation of the Earth. The major differentiation processes occurring in subduction zones are dehydration and/or partial melting within the subducted lithosphere. The distinctive arc magma chemistries, i.e., LILE enrichment relative to HFSE, a steeper array in a Pb-Pb diagram, negative or positive correlation in a Nd-Sr diagram, *etc.*, have been attributed to the overprinting of SDSC to the original mantle wedge throughout these reactions (e.g. Gill, 1981; Hawkesworth et al., 1993; Pearce and Peate, 1995; Tatsumi and Eggins, 1995). However, the distinct nature and the particular origin of SDSC still lie at the heart of recent debates on the processes responsible for isotope and trace element geochemistry of subduction related magmas.

The combination of the isotopic ratios, the trace element compositions and the H_2O concentrations of subduction zone lavas may provide a key constraint on the above problems, because these would suggest the sources of SDSC, processes of SDSC generation and the amount of added SDSC to the arc magma source, respectively. In this point of view, the Setouchi volcanic rocks would be the most suitable samples to constrain above problems, because primitive HMAs and basalts, which formed with different H_2O contents, had erupted simultaneously at the same region (e.g. Tatsumi 1982).

Japan Sea is a back-arc basin situated behind the SW and NE Japan

arcs. Based on paleomagnetic and K-Ar age data, Japan Sea is inferred to be formed during 20-13 Ma, accompanying the rapid rotational movement of the SW Japan arc sliver at the late stage of spreading, i.e., 15-13 Ma (e.g., Otofuji et al., 1983, 1985, 1987, 1991; Kaneoka et al 1990, 1992; Ishikawa et al., 1996). The geochemical influence of Japan Sea opening upon magmatism on the NE Japan arc were extensively studied (e.g., Nohda and Wasserburg, 1986; Nohda et al., 1988; Tatsumi et al., 1988, 1990, 1994). These authors concluded that the chemical characteristics of the mantle wedge beneath the back-arc side of the NE Japan arc changed from less to more depleted during the back-arc opening which would be caused by injection of depleted asthenospheric mantle materials into mantle wedge. SW Japan arc sliver had drifted southward about 600 km for about only 1 Ma (Otofuji and Matsuda, 1987; Ishikawa et al., 1996). This drastic movement would change the mantle structure beneath SW Japan arc. Nevertheless, the effect of this mega-tectonic event upon the mantle wedge beneath SW Japan have not been investigated. It has been suggested that magmatism in the Setouchi volcanic belt had took place contemporary with the rotation of SW Japan sliver. Moreover, some Setouchi volcanic rocks have been inferred to be derived directly from the upper mantle (e.g., Tatsumi, 1982). Therefore, analyses of the Setouchi volcanic rocks should give essential constraints on geochemical evolution of the sub-Setouchi mantle wedge during the rotation of SW Japan sliver. The major goal of this thesis is to document the nature of overprinted SDSC and to evaluate the relation of the Setouchi volcanism

and the rotational movement of SW Japan sliver at the late stage of the Japan Sea opening on the basis of the geochemistry of the Setouchi volcanic rocks.

Tectonic setting

The Setouchi volcanic belt was built along the SW Japan arc, where the Eurasian plate overlies the subducted Philippine Sea plate. It occupies the narrow zone for about 600 km parallel both to the Nankai Trough and Median Tectonic Line, and can be divided into eight subprovinces (Fig. 1); HMAs occur in the central four. The volcanic belt consists of dacitic and rhyolitic pyroclastic flows, dissected andesitic stratovolcanos and many monogenic volcanoes including small lava flows and dikes.

The following five features may characterize for the Setouchi volcanism: (1) the volcanism was short-lived (about 1 Ma; Anno, 1994; Ishikawa et al., 1996; Tatsumi et al., 1996), (2) it is located in the present forearc region (Fig. 1), (3) the subducted plate was very young, as the Shikoku Basin formed at the 27-17 Ma (e.g., Kobayashi and Nakada, 1978; Shih 1980), (4) the occurrence of plagioclase-free, relatively aphyric basalts and andesites (sanukitoids) which include HMAs (Tatsumi and Ishizaka, 1981), (5) andesites, both HMAs and evolved porphyritic andesites, show a typical calc-alkaline trend (Tatsumi and Ishizaka 1981). The zonal distribution of the volcanic belt and the occurrence of calc-alkaline rocks suggest that the Setouchi volcanism is a subduction-related phenomena, as

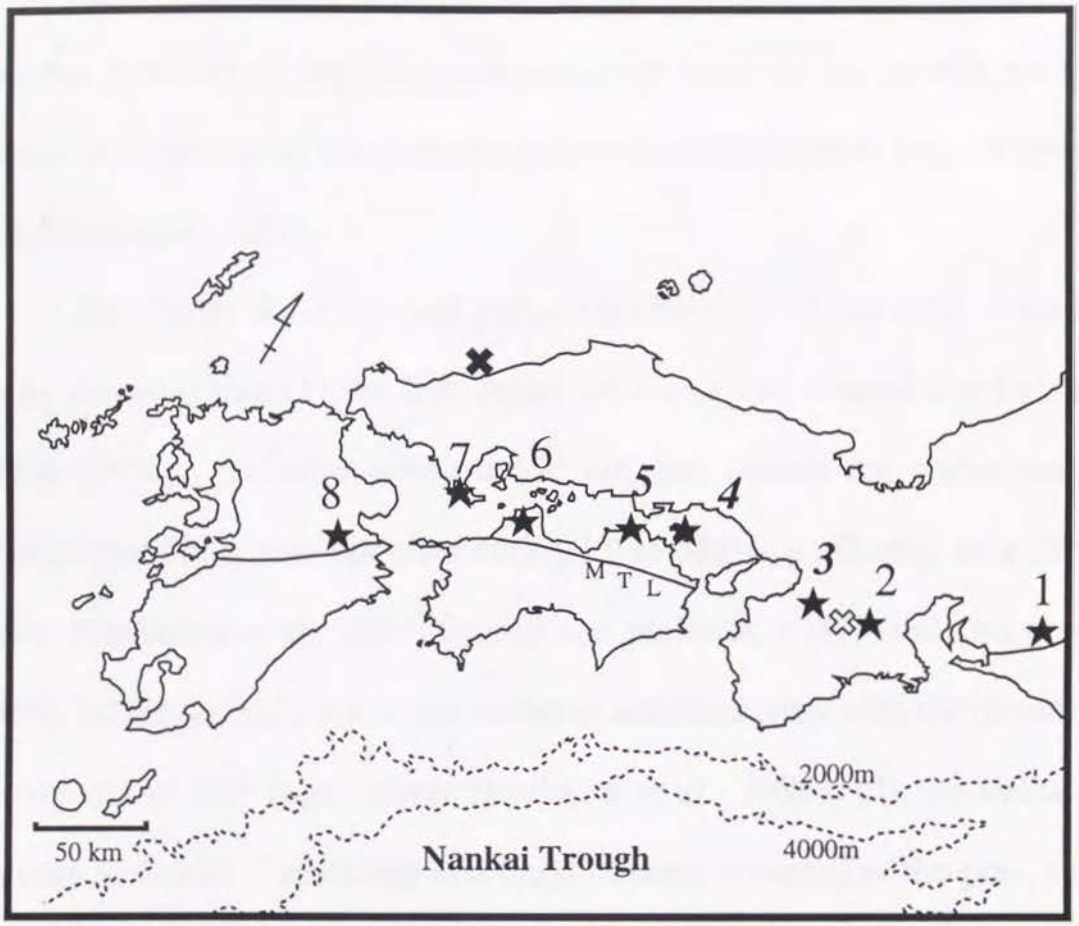

★ **Setouchi Volcanic Rocks**

1. Shidara	6. Matuyama
2. Muro	7. Yamaguti
3. Osaka	8. Ohita
4. Shodo-Shima	
5. Takamatsu	

✖ Granulitic xenolith

⊠ Upper crustal material

Fig.1. Distribution of Setouchi volcanic rocks in SW Jpan.

is the case of general orogenic andesites. However, the unusual conditions, i.e., the presence of high temperature in the sub-fore arc mantle wedge, would be essential in the genesis of the Setouchi magmas (e.g., Tatsumi and Maruyama, 1989).

The recent K-Ar age and paleomagnetic data of Setouchi volcanic rocks revealed that (1) the SW Japan arc sliver had rotated clockwisely about 60°, i.e., drifted southward 500 km, and caused the obduction of newly-bone Philippine Sea plate during 13-15 Ma (e.g., Otofuji et al 1985, 1991; Hayashida et al., 1988; Otofuji and Matsuda, 1987; Ishikawa et al., 1996). (2) the Setouchi volcanism occurred simultaneously with the rotational movement of SW Japan sliver (Ishikawa et al., 1996), (3) the volcanic activity in Osaka, Takamatsu and Shodo-Shima occurred at the pre-, syn- and post-rotational stage, respectively (Ishikawa et al., 1996), (4) felsic volcanism preceded intermediate and mafic eruptions in each area (Anno, 1995), (5) both the rotation of SW Japan sliver and the Setouchi volcanism occurred at the late stage of Japan Sea opening (Jolivet and Tamaki, 1992; Ishikawa et al., 1996).

Geology

Shodo-Shima area

On the Shodo-Shima island, is located a dissected stratovolcano of Setouchi volcanics on the basement Ryoke complex (Fig. 2). The Miocene strata in the Shodo-Shima island are divided into two groups, i.e., the

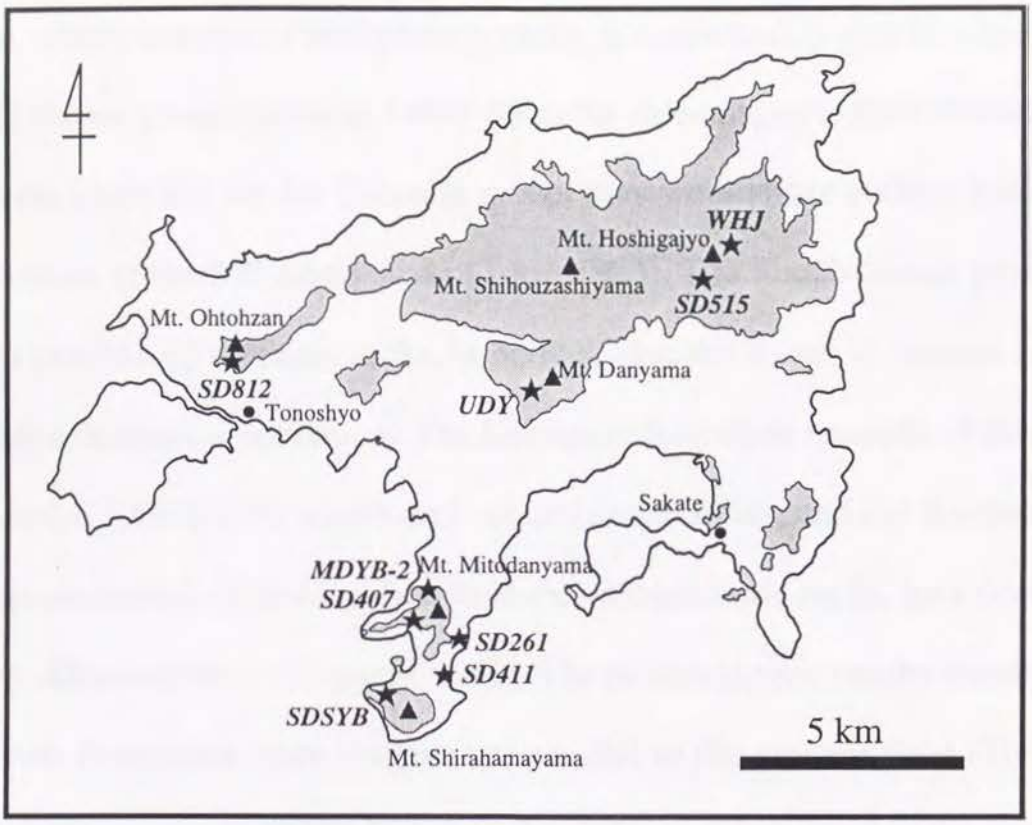

Fig. 2. Locality map of the samples in Shodo-Shima area. Distribution of the Setouchi volcanic rocks is also shown (hatched areas).

Tonosho group and Shodo-Shima group in ascending order. The Tonosho group, which consists of sedimentary rocks, is conformably overlain by the Shodo-Shima group (Tatsumi, 1983). Since the paleomagnetic field deflected eastward about 60° for the Tonosho group, they would have bedded before the rotation of the SW Japan sliver (Torii, 1983). The Shodo-Shima group, which consists of volcanic rocks, is divided into the lower Uchinomi and the upper Kankakei formation. The Uchinomi formation consists of felsic lava rocks, lava domes, sheets and volcaniclastic flows, and the Kankakei formation consists of intermediate to mafic volcaniclastic rocks, lava flows, stocks, dikes and necks (Tatsumi, 1983). The paleomagnetic results revealed that both formations were magnetized parallel to the modern field (Torii, 1983; Ishikawa et al., 1996). K-Ar age determination indicate that the mean age of the Uchinomi formation and the Kankakei formation are 13.78 ± 0.17 and 12.82 ± 0.12 Ma, respectively (Anno, 1995). It is thus suggested that the volcanism in Shodo-Shima occurred immediately after the rotation of SW Japan sliver.

Takamatsu area

The Miocene volcanic stratum in E. Shikoku is the Sanuki group (Saito, 1962). These volcanic rocks comprising mesas, buttes and dissected hills are distributed unconformably on the basement Ryoke complex (Fig. 3). Among these, Goshikidai and Kokubudai, which occupy the central part of this region, are the largest volcanic mass composed mainly of andesitic

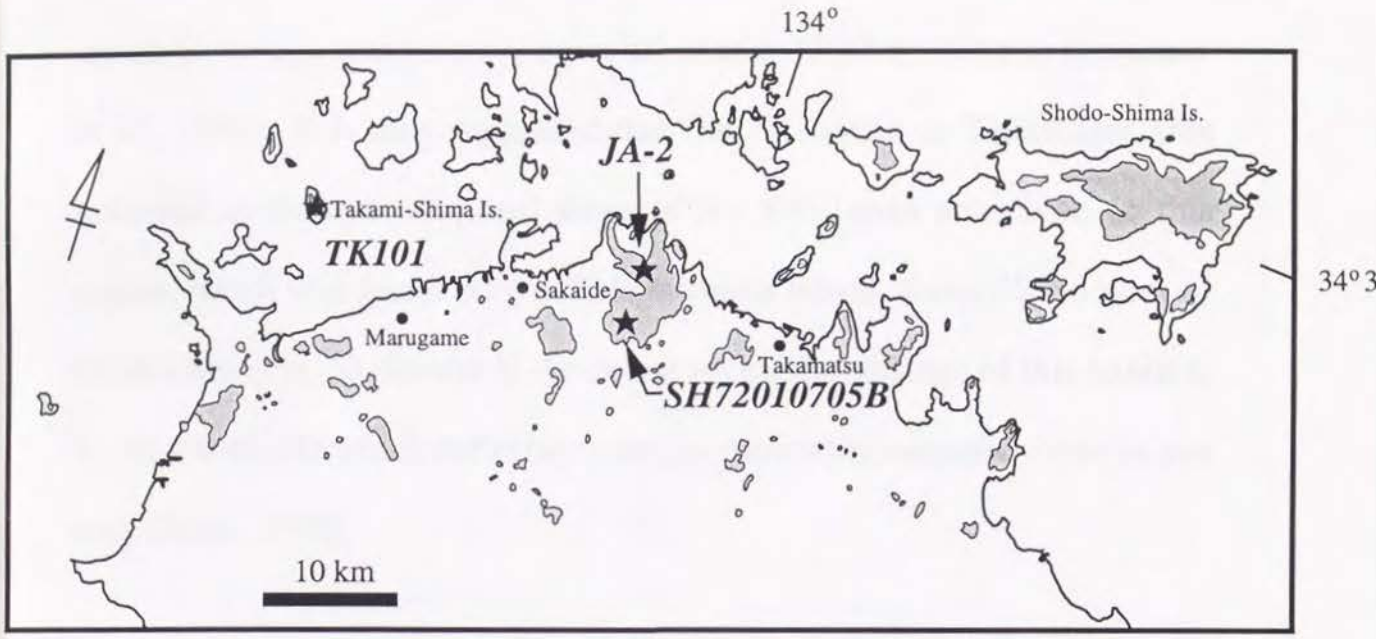

Fig. 3. Locality map of samples in Takamatsu area in NE. Shikoku. Distribution of the Setouchi volcanic rocks is also shown (hatched areas).

sanukitoids. The Sanuki group are divided into the lower Higasioku formation and the upper Kokubudai formation (Sato, 1982). A clockwise deflection in declination (D = 21.4° ± 9.9) was observed in Kokubudai formation of which K-Ar age was recently revealed, that is 13.39 ± 0.21 Ma (Ishikawa et al., 1996). It is thus suggested that the volcanism in Takamatsu area occurred at the syn-rotational stage of the SW Japan arc sliver. In this region, basalt was found only in Takamishima island, about 25 km west of Goshikidai (Fig. 3). Recent K-Ar dating reveal that the age of this basalt is 11.96 ± 0.45 Ma which definitely younger than other volcanic rocks in this area (Anno, 1995).

Osaka area

In the Osaka area, dikes and necks sporadically intrude into the basement Ryoke complex (Fig. 4). Recent K-Ar age determination documented that ages of Sionomiya, Teragaike, Sigisan volcanic rocks are 14.51, 14.13 and 13.92 Ma, respectively and are distributed between the age of Muro welded tuff (14.86 ± 0.32 Ma) and that of Takamatsu volcanic rocks (13.39 ± 0.21 Ma). Since the Muro and Takamatsu volcanic rocks erupted pre-rotation and syn-rotation of SW Japan sliver, respectively (Torii, 1983; Ishikawa et al., 1996), it is suggested that the volcanism in Osaka area took place at pre-rotation stage or immediately after the commencement of the rotation of the SW Japan arc sliver.

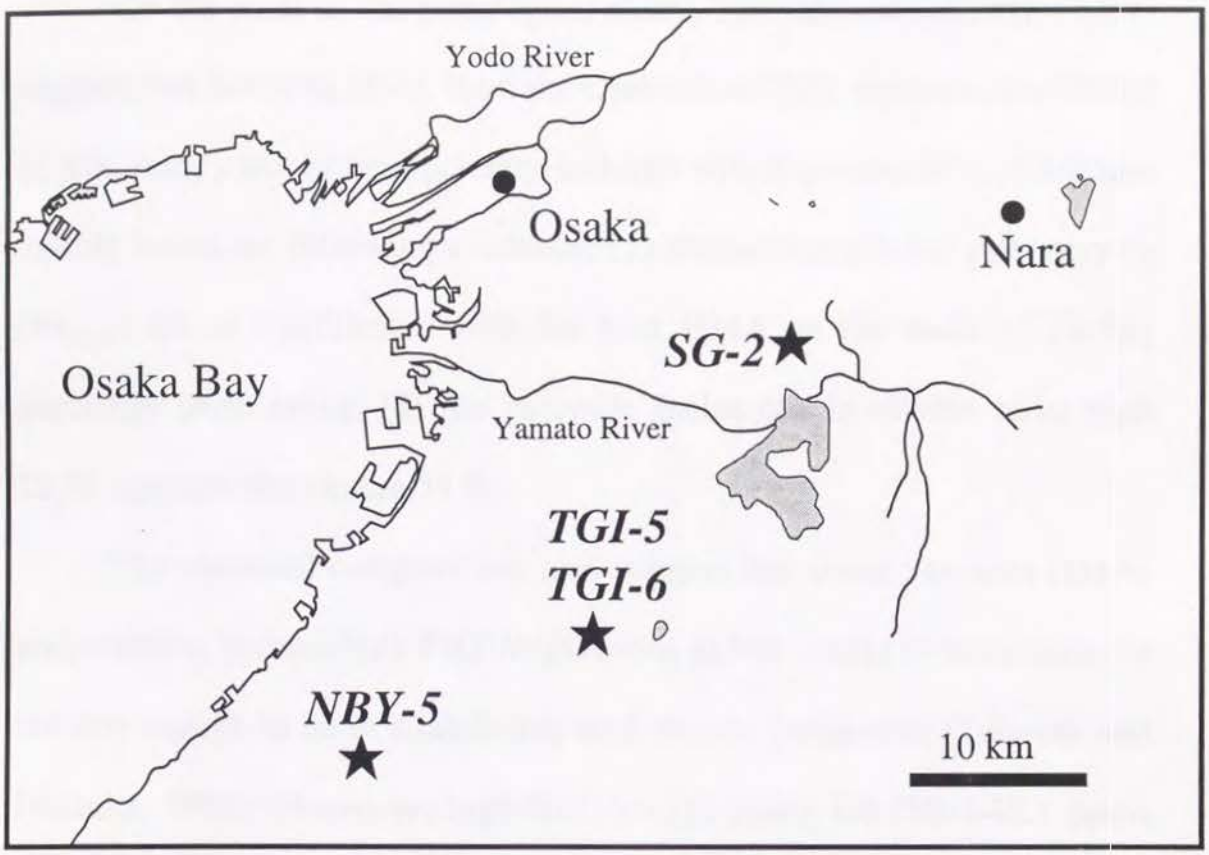

Fig. 4. Locality map of the samples in Osaka area. Distribution of the Setouchi volcanic rocks is also shown (hatched areas).

Experimental petrology and mineralogy

On the basis of the petrological study, Tatsumi and Ishizaka (1981) suggest that Setouchi HMA from the Osaka area (TGI, equivalent to TGI-5 in this study) would be a primary andesite which generated in the upper mantle based on following evidence: (1) magnesian olivine phenocrysts (Fo_{87-91}) are in equilibrium with the host HMA on the basis of Fe-Mg exchange partitioning, (2) the chromite inclusions in olivine have high Cr_2O_3 contents (maximum 55 %).

The chemical compositions also suggest that some Setouchi HMAs are primitive, because bulk FeO*/MgO ratios (0.546-0.931) of these andesite are low enough to be in equilibrium with mantle peridotites (Tatsumi and Ishizaka, 1982). Moreover, high Ni (101-312 ppm), Co (30.0-45.1 ppm) and Cr (208-756 ppm) contents of HMAs also suggest that these andesite were produced by direct partial melting of mantle peridotites (Tatsumi and Ishizaka, 1982). Based on the petrographic observations of the basalt and HMA, Tatsumi and Ishizaka (1982) demonstrated that the andesite could not be derived from a basaltic magma by fractional crystallization and concluded that the andesite and basalt were generated independently in the mantle beneath SW Japan.

On the basis of high pressure melting experiments on an augite olivine andesite (SD261) and a basalt (SD438, equivalent to SDSYB in this study), Tatsumi (1982) examined the following possible mechanisms for simultaneous production of primary basaltic and andesitic magmas; (1)

basalt and HMA magmas were formed at an identical depth by different degrees of partial melting; (2) basaltic magmas were generated in the presence of much smaller amount of H_2O in their source region than HMA magma; (3) basaltic magmas can be produced at a greater depth than HMA magmas. He concluded that (2) would be the plausible model, because hypothesizing that the amounts of H_2O in basalts magma source are identical to those for HMAs is not realistic.

Samples

Twenty volcanic rocks were selected for the isotopic analysis from the three volcanic fields, namely, Osaka, Takamatsu and Shodo-Shima area (Fig. 1).

Shodo-Shima area

Most samples used in this study are from the Kankakei formation on Shodo-Shima island (Fig. 2), because extensive petrographic, high pressure melting experimental, paleomagnetic studies and K-Ar age determination were conducted for these rocks (e.g., Tatsumi and Ishizaka 1982 a, b; Tatsumi, 1982; Anno, 1995; Ishikawa et al., 1996). Based on these studies, it is inferred that the HMA SD261 and the basalt SDSYB have chemical compositions of the primary magma generated in the upper mantle (Tatsumi, 1982). All HMA in this area are augite-olivine HMA of which mantle residual phase assemblages were inferred to be lherzolitic as well as basalt

(Tatsumi, 1982).

Takamatsu area

Two HMAs and a basalt were selected for this study. HMA JA-2, i.e., JSG (Geological Survey of Japan) standard rock sample, and SH72010705B were collected from Goshikidai and Kokubudai, respectively in central part in this area (Fig. 3). The basalt sample TK101 was collected in Takamishima island (Fig. 3).

Osaka area

From this area, five HMAs were chosen for this study (Fig. 4). One of HMA, i.e., TGI-5, has a chemical composition approximating that of the primary magma generated in the upper mantle (Tatsumi, 1981). The NBY-5 has a low FeO*/MgO ratio and high Ni content. This suggest that it would also equilibrate with mantle peridotite. The HMAs in this area are bronzite-olivine HMA, and were inferred that the mantle residual phase assemblages were harzburgitic (Tatsumi, 1981). There is no primitive basaltic rock in this region.

Sediments

The terrigenous sediments, i.e., turbidites ~ 560 m thick, were recovered from the floor of the Nankai Trough at the Site 582, DSDP Leg 87 (Fig. 5), and details were discussed elsewhere (Taira and Niitsuma

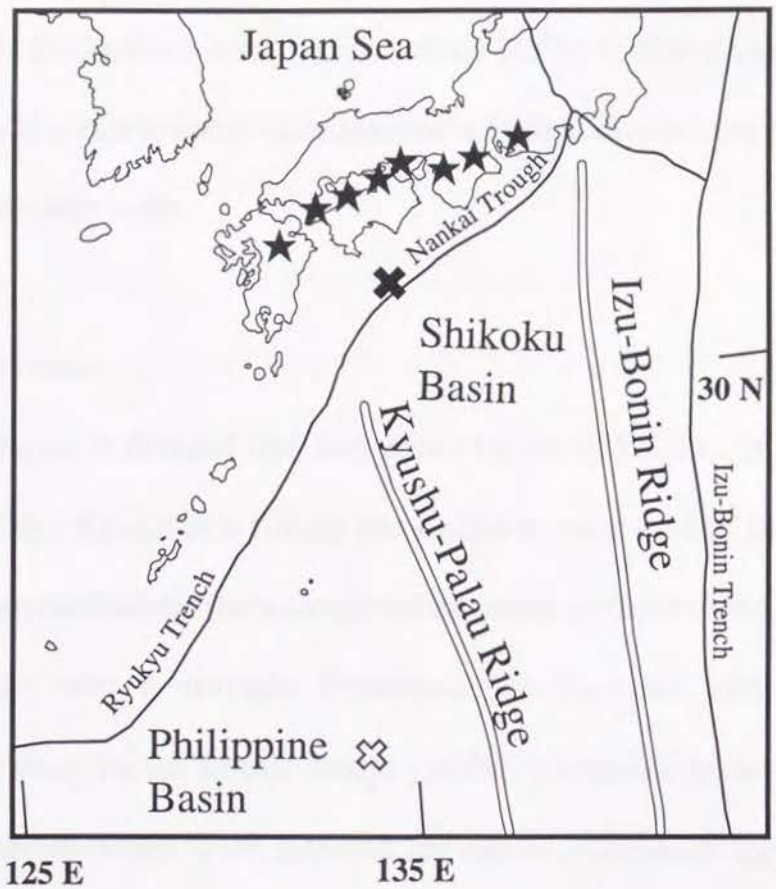

Fig.5. Distribution of the Setouchi volcanic rocks and locality of the sediments.

1985). The pelagic sediments were recovered from the central Philippine sea (DSDP 15-12), the location is indicated in Fig 5. These sediments were selected for the representative sediments which had subducted beneath the Setouchi volcanic zone.

Crustal materials

SW Japan is divided into two zones by the MTL, i.e., Inner zone and the Outer zone. Ryoke belt situate the southern most part in the Inner zone which is characterized by the widespread exposure of Cretaceous to Paleogene acidic rocks which intrude Paleozoic to Jurassic sedimentary or metasedimentary rocks. In this study, granite, gneissose granite and gneiss of metasediment origin were selected for representative of upper crust. All of these rocks were collected in the Nara prefecture 50 km eastward of Osaka area (Fig. 1). A granulitic xenolith from the Utashima Island in Yamaguchi prefecture was also analyzed as a possible candidate of lower crust (Fig. 1).

Analytical procedures

Chemical procedure

Rock chip samples weighted about 100 mg were washed by acetone utilizing ultrasonic bath three times, and rinsed by pure water several times. Then, these were warmed (70-80 °C) by 6 N HCl for 30-60 minutes to eliminate surface contamination. Subsequently, samples were decomposed

by a mixture of 1 ml of 20 N HF and 1 ml of 14 N HNO_3 with few drops of 10 N $HClO_4$ in screw-top PFA® teflon vials at 90 °C for 3-7 days. Dicomposed samples were dried completely and then converted to chloride form for chemical sepraion.

Samples in chloride form were dissolved completely with 3 ml of 1N HBr and loaded onto columns (3 mm id × 30 mm) packed with anion exchange resin (Bio-Rad AG-1X8® 100-200 mesh). Then, the colums were washed with 2 ml HBr. These eluents were recovered for Nd and Sr isotopic analyses. Subsequently, Pb were eluted with 2 ml of 6 N HCl. Further, Pb purification were performed by the use of same columns with basicaly same method described above. Finally, purified Pb samples were dissolved to a drop of 14 N HNO_3 to burn out orgenic matter and dried to convert nitric form.

Samples for Nd and Sr isotopic analyses in bromide form were converted to chloride form and then dissolved to 1 ml of 1 N HCl and loaded onto columns (10 mm id × 200 mm) packed with cation exchange resin (Bio-Rad AG-X12® 200-400 mesh). The colums were washed with 40 ml of 2 N HCl. Then, Sr were recovered with 20 ml of 2 N HCl. Subsequently, LREE were collected with 20 ml of 4 N HCl after washing columns by 20 ml of 4 N HCl. Sr and LREE purification were conducted by the usage of smaller column (7 mm id × 140 mm) packed with cation exchande resin (Bio-Rad AG-X8® 200-400 mesh) with 2 N HCl and 4 N HCl as eluates, respectively. Nd and Sm separation were performed by the

HDEHP + teflon columns (6.5 mm id × 200 mm) with 0.2 N HCl eluantes. Current total procedure blank levels for Pb, Sr and Nd were 60 pg, 100 pg and 30 pg, respectively and are negligible for the samples studied here.

Mass Spectrometry

Pb, Nd and Sr isotopic compositions were measured using a Finigan® MAT 261 mass spectrometer at Kyoto Sangyo University with Re single, Re-Ta double and Ta single filament mode, respectively. The accelerating voltage was adjusted to 10 kV. Collecter system is a single Faraday cup with a resistance of 10^{11} Ω. The data aquisitions were made by peak jumping. The raw data were processed for baseline correction and bilinear correction by on-line system with Hewlett-Packard HP 9133 computer. Prior to sample loading , the Re and Ta filaments were outgassed for 30 minuites at filament current of 4.0 A at 10^{-6} Torr.

200-500 ng of Pb per sample was loaded onto Re filament with silica-gel and H_3PO_4 activator. The ^{208}Pb signal were generally arround 1-2 × 10^{-11} A. To correct mass fractionation effects and check reproducibility, repeated analyses of external standard NBS SRM 981 lead were conducted. The averages and standard deviations of 17 separated analyses of $^{206}Pb/^{204}Pb$, $^{207}Pb/^{204}Pb$ and $^{208}Pb/^{204}Pb$ are 16.900 ± 0.005, 15.463 ± 0.007 and 36.529 ± 0.020, respectively. Based on these results, upward correction factors per amu for $^{206}Pb/^{204}Pb$, $^{207}Pb/^{204}Pb$ and $^{208}Pb/^{204}Pb$ are determined, those are, 0.11 %, 0.11 % and 0.13 %, respectively. Because, there is no way for

fractionation correction in case of Pb isotope analyses and the environmental contamination during sample preparation severely effect upon Pb isotope measurement, special care were taken to obtain precise Pb isotopic compositions. Details of Pb analitical procedure is given Appendix 1.

300-700 ng of Nd per sample was loaded onto Ta filament with 1 μl of 1 N H_3PO_4. Nd isotopic compositions were measured by Re-Ta double filaments mode at ion intensities of $^{144}Nd = 3\text{-}5 \times 10^{-12}$ A. Results were normalized to $^{146}Nd/^{144}Nd = 0.7219$. The La Jolla standard value of single analysis in this study was 0.511833 ± 26.

1-2 μg of Sr per sample were loaded onto single Ta filament with 1 μl of 1 N H_3PO_4. The ^{88}Sr signal was generally around $1\text{-}2 \times 10^{-11}$ A. Results were normalized to $^{86}Sr/^{88}Sr = 0.1194$. The value of NBS SRM 987 of single analysis and the value of the Eimer & Amend standard of single analysis were 0.710171 ± 24 and 0.708009 ± 24, respectively.

Major and trace elements

Major and trace elements were analyzed using RIGAKU® Symaltics 3550 and 3070 X-ray fluorescence (XRF) spectrometers in Kyoto University on fused glass beads and pressed powder pallets, respectively. Details of counting times, operating conditions and detection limits can be found in Goto and Tatsumi (1991, 1992). Analytical errors for trace elements are better than 5%, except Pb (7%).

From this set of samples, 9 samples were further analyzed for REE

(Rare Earth Elements) by ICP (inductivity coupled plasma) in Kyoto University.

Results

The major and trace element data for analyzed samples are given in Table 1, the REE (Rare Earth Element) data shown in Table 2, and the isotopic composition determined in this study, along with previously reported were shown in Table 3.

FeO*/MgO ratios of the selected basalts and the HMAs are less than unity (Table. 1), suggesting that they could equilibrate with mantle olivine on the basis of Fe-Mg partitioning. Therefore, basalts and HMAs used in this study would be primitive, and enable to infer the chemical and isotopic compositions of the mantle beneath the Setouchi volcanic belt.

The Setouchi volcanic rocks have trace element characteristics which typify subduction related rocks (Fig. 6); an element with larger ionic radius is more enriched when comparing elements with an identical charge. A clear exception is Pb, which is strongly enriched in HMAs. The LILE concentrations of Setouchi volcanic rocks are about ten to a hundred times higher than those of the N-type MORB and are also higher than those of the basalts in same area (Table 1, Fig. 6). The TiO_2 and Zr concentrations of the Setouchi volcanic rocks are similar to those of N-type MORB (Sun and McDough, 1989), but the Nb contents of HMAs are relatively higher than those of N-type MORB and the basalt in same area (Table 1, Fig. 6).

Table 1. Major and trace elements compositions of representative Setouchi volcanic rocks, terrigenous sediments and pelagic sediments.

Location	Shodo-Shima						
sample rock type	SDSYB basalt	SD-261 HMA	SD407 HMA	SD411 HMA	SD812 HMA	MDYB-2 HMA	UDY porphyric andesite
SiO_2 (wt. %)	48.95	55.37	56.12	55.80	56.33	57.31	59.07
Al_2O_3	14.69	15.55	15.38	15.41	16.48	15.81	17.98
CaO	8.75	7.04	6.87	6.92	6.97	6.46	5.62
$Fe_2O_3^*$	10.21	6.92	6.87	6.84	6.19	6.43	6.35
K_2O	1.20	2.25	2.38	2.42	2.04	2.28	2.37
MgO	11.79	6.89	7.61	7.77	7.19	6.24	2.83
MnO	0.17	0.17	0.14	0.14	0.11	0.14	0.12
Na_2O	2.57	2.84	2.87	2.64	3.06	3.12	3.43
P_2O_5	0.27	0.17	0.16	0.16	0.16	0.17	0.24
TiO_2	1.02	0.65	0.62	0.61	0.61	0.59	0.64
TOTAL	99.60	97.85	99.03	98.71	99.15	98.55	98.65
FeO^*/MgO	0.78	0.90	0.81	0.79	0.78	0.93	2.02
Ba (ppm)	219	195	211	213	263	221	346
Nb	4	5	4	4	5	5	6
Ni	207	148	132	126	151	123	15
Pb	8.3	17.4	18.3	17.7	17.8	17.9	13.9
Rb	33.2	113.6	119.3	121.3	68.4	120.6	147.7
Sr	277	267	249	253	299	274	362
Th	4.2	4.8	4.7	4.6	5.3	6.2	6.1
Y	18	15	16	16	13	16	31
Zr	99	80	82	82	109	92	132

$Fe_2O_3^*$ and FeO^*, total irons as Fe_2O_3 and FeO, respectively.

Table 1. (continued)

Location	Shodo-Shima		Takamatsu				
sample rock type	SDWHJ porphyric andesite	SD515 porphyric andesite	TK101 basalt	SH7201 HMA	JA-2 HMA	TK6` porphyric andesite	TK-KAN porphyric andesite
SiO_2 (wt. %)	55.04	56.56	50.27	55.46	56.18	64.96	63.67
Al_2O_3	16.20	17.85	17.06	15.54	15.32	17.52	17.55
CaO	6.97	6.65	9.00	6.94	6.48	3.76	4.24
$Fe_2O_3^*$	8.17	7.10	7.92	6.71	6.95	3.80	4.17
K_2O	1.75	2.08	0.58	1.63	1.80	2.86	2.74
MgO	7.07	4.36	8.76	9.33	7.68	1.53	2.15
MnO	0.14	0.12	0.13	0.13	0.11	0.09	0.09
Na_2O	2.91	3.17	3.22	2.90	3.08	4.25	4.20
P_2O_5	0.21	0.23	0.14	0.16	0.15	0.22	0.23
TiO_2	0.68	0.78	0.95	0.70	0.67	0.50	0.56
TOTAL	99.14	98.90	98.04	99.50	98.42	99.48	99.59
FeO^*/MgO	1.04	1.47	0.81	0.65	0.81	2.24	1.74
Ba (ppm)	233	297	95	288	317	453	439
Nb	3	5	2	8	10	10	10
Ni	117	25	124	132	142	14	18
Pb	12.1	11.8	4.3	17.7	19.3	33.4	31.7
Rb	99.5	112.8	19.2	60.5	68.0	128.1	120.4
Sr	347	406	223	245	252	282	293
Th	3.4	4.8	1.6	4.5	4.7	11.2	10.9
Y	19	17	19	16	18	15	15
Zr	105	116	96	107	119	229	219

Table 1. (continued)

Location	Osaka				Nankai Trough Site 582, DSDP Leg 87		
sample rock type	TGI-5 HMA	NBY-5 HMA	SG-2 HMA	NJSB HMA	T-1 turbidite	T-2 turbidite	T-3 turbidite
SiO_2 (wt. %)	57.27	55.77	51.87	53.75	61.89	65.50	64.49
Al_2O_3	14.26	13.98	15.48	16.62	18.28	16.46	17.47
CaO	6.31	6.96	8.14	8.18	2.32	2.65	1.80
$Fe_2O_3^*$	6.19	6.81	8.29	7.94	7.60	6.10	6.65
K_2O	1.16	1.20	0.97	1.17	3.39	2.63	3.16
MgO	9.45	10.93	9.54	6.64	2.90	2.43	2.60
MnO	0.12	0.13	0.14	0.15	0.13	0.10	0.09
Na_2O	2.57	2.36	2.57	2.87	2.17	2.71	2.46
P_2O_5	0.10	0.09	0.12	0.18	0.16	0.14	0.40
TiO_2	0.42	0.39	0.76	1.08	0.80	0.73	0.77
TOTAL	97.85	98.62	97.88	98.60	99.65	99.46	99.89
FeO^*/MgO	0.59	0.56	0.78	1.08	2.36	2.26	2.30
Ba (ppm)	336	378	233	275	490	440	456
Nb	3	2	3	5	10	8	10
Ni	179	254	194	32	46	34	41
Pb	13.1	11.2	9.0	13.6	27.5	17.7	21.9
Rb	44.7	47.5	36.5	41.8	130.6	96.7	124.1
Sr	308	284	274	301	165	207	183
Th	4.9	3.0	2.3	3.8	13.1	9.3	12.0
Y	11	11	14	18	27	22	23
Zr	94	68	80	116	153	156	161

Table 1. (continued)

Location	Nankai Trough Site 582, DSDP Leg 87						
sample rock type	T-4 turbidite	T-5 turbidite	T-6 turbidite	T-7 turbidite	T-8 turbidite	T-9 turbidite	T-10 turbidite
SiO_2 (wt. %)	64.03	64.00	63.24	67.50	63.36	65.62	63.34
Al_2O_3	17.81	17.82	18.00	16.08	18.40	16.23	18.12
CaO	2.29	2.33	2.54	2.54	1.79	3.62	1.48
$Fe_2O_3^*$	6.89	6.56	7.02	5.44	7.06	6.12	7.59
K_2O	3.06	2.90	2.87	2.59	3.07	2.21	3.17
MgO	2.60	2.69	2.96	2.23	2.88	2.55	2.77
MnO	0.11	0.11	0.11	0.10	0.09	0.10	0.09
Na_2O	2.41	2.52	2.45	2.63	2.44	2.75	2.37
P_2O_5	0.16	0.16	0.16	0.13	0.19	0.13	0.15
TiO_2	0.78	0.77	0.79	0.68	0.80	0.69	0.78
TOTAL	100.15	99.86	100.14	99.91	100.08	100.03	99.87
FeO^*/MgO	2.38	2.19	2.14	2.20	2.21	2.16	2.46
Ba (ppm)	443	401	387	395	438	400	501
Nb	10	9	8	8	10	6	9
Ni	38	37	36	29	36	28	36
Pb	22.9	22.1	22.4	15.6	23.2	13.9	23.8
Rb	120.1	112.2	111.6	97.7	120.9	82.2	124.7
Sr	176	177	177	205	163	238	144
Th	12.7	10.5	10.6	8.1	11.5	7.6	11.2
Y	25	24	25	20	24	19	23
Zr	160	157	147	156	152	135	145

Table 1. (continued)

Location		Philippine Sea GDP15-12					
sample rock type	T-COM turbidite (composite)	P-1 pelagic clay	P-2 pelagic clay	P-3 pelagic clay	P-4 pelagic clay	P-5 pelagic clay	P-6 pelagic clay
SiO_2 (wt. %)	64.36	63.82	58.89	58.36	58.60	59.50	58.73
Al_2O_3	17.47	16.40	18.32	18.57	19.18	19.65	19.45
CaO	2.36	1.75	1.77	1.66	1.46	1.56	1.89
$Fe_2O_3^*$	6.69	6.13	8.47	8.78	8.85	9.25	8.13
K_2O	2.89	3.57	3.44	3.46	3.43	3.40	3.24
MgO	2.69	2.26	3.16	3.26	3.30	3.34	2.85
MnO	0.10	0.54	0.80	0.69	0.73	0.81	0.76
Na_2O	2.42	4.65	3.97	3.87	3.73	3.74	4.17
P_2O_5	0.18	0.20	0.24	0.23	0.21	0.23	0.26
TiO_2	0.76	0.61	0.87	0.90	0.90	0.92	0.81
TOTAL	99.93	99.95	99.94	99.76	100.38	102.43	100.29
FeO^*/MgO	2.24	2.44	2.41	2.42	2.41	2.49	2.56
Ba (ppm)	449	886	822	866	787	782	744
Nb	9	9	12	12	12	12	11
Ni	37	59	91	81	83	82	68
Pb	21.5	36.1	46.0	43.0	44.6	47.1	48.5
Rb	111.8	123.6	128.3	130.0	137.3	132.1	117.3
Sr	183	188	204	204	190	195	214
Th	10.8	13.9	14.4	14.6	15.6	14.9	15.3
Y	23	33	41	38	37	41	47
Zr	152	164	181	176	175	177	197

Table 1. (continued)

Location	Philippine Sea GDP15-12						
sample rock type	P-7 pelagic clay	P-8 pelagic clay	P-9 pelagic clay	P-10 pelagic clay	P-11 pelagic clay	P-12 pelagic clay	P-COM pelagic clay (composite)
SiO_2 (wt. %)	58.03	57.69	58.91	58.28	58.16	57.92	59.11
Al_2O_3	18.88	19.52	19.52	19.02	19.03	18.93	18.84
CaO	1.58	1.51	1.25	1.30	1.30	1.32	1.53
$Fe_2O_3^*$	9.05	9.19	8.51	8.92	8.96	8.93	8.59
K_2O	3.46	3.36	3.59	3.65	3.65	3.66	3.50
MgO	3.25	3.28	3.17	3.21	3.19	3.25	3.11
MnO	0.73	0.79	0.63	0.69	0.71	0.73	0.72
Na_2O	3.84	3.95	3.47	3.53	3.62	3.84	3.70
P_2O_5	0.22	0.22	0.20	0.22	0.23	0.23	0.22
TiO_2	0.91	0.91	0.87	0.91	0.90	0.90	0.87
TOTAL	99.94	100.42	100.12	99.73	99.75	99.70	100.19
FeO^*/MgO	2.51	2.52	2.42	2.50	2.53	2.47	2.48
Ba (ppm)	813	788	769	837	874	855	665
Nb	12	11	13	13	13	12	12
Ni	81	80	77	78	80	79	72
Pb	43.9	45.8	42.5	45.4	45.6	46.1	43.5
Rb	129.4	124.6	136.9	138.5	138.1	136.4	128.1
Sr	206	196	180	187	188	190	190
Th	14.9	14.5	16.4	15.7	16.0	15.7	14.8
Y	37	40	34	40	41	42	38
Zr	176	172	182	180	180	180	174

Table 1. (continued)

Location	Nabari, Nara Prefecture					Uta-Shima, Yamaguchi Prefecture
sample rock type	NBN-1 gneiss	SR-1 gneissose granite	SR-2 gneissose granite	NBR2-3 granite	KUZ-2 granite	U-X granulite (xennolith)
SiO_2 (wt. %)	66.61	67.84	49.95	76.89	74.60	48.50
Al_2O_3	16.41	15.61	17.45	13.59	14.53	22.01
CaO	2.90	3.86	7.30	1.86	1.76	10.67
$Fe_2O_3^*$	4.63	4.54	13.34	1.30	1.53	9.71
K_2O	3.54	1.99	1.70	3.18	3.30	0.11
MgO	1.65	1.89	4.39	0.30	0.24	3.71
MnO	0.12	0.09	0.23	0.03	0.07	0.16
Na_2O	3.40	3.34	1.31	3.36	3.83	3.21
P_2O_5	0.15	0.16	1.03	0.05	0.05	0.20
TiO_2	0.60	0.63	3.16	0.12	0.12	1.18
TOTAL	100.01	99.98	99.87	100.67	100.03	99.46
FeO^*/MgO	2.52	2.16	2.73	3.83	5.86	5.86
Ba (ppm)	544	320	122	1157	435	55
Nb	9	8	84	6	10	2
Ni	29	14	4	4	4	1
Pb	25.5	7.9	6.6	24.1	26.9	3.0
Rb	114.2	91.0	47.7	77.9	97.0	0.7
Sr	358	241	486	347	241	562
Th	9.2	-0.5	6.3	5.0	4.8	0.3
Y	23	8	48	11	19	10
Zr	183	142	436	143	109	27

Table 2. REE compositions of representative
Setouchi volcanic rocks, terrigenous sediments and pelagic sediments.

Location	Shodo-Shima		Osaka		Nankai Trrogh	Philippine Sea
sample	SDSYB	SD261	TGI-5	SG-2	T-COM	P-COM
rock type	basalt	HMA	HMA	HMA	turbidite (composite)	pelagic clay (composite)
La (ppm)	10.3	8.6	12.0	8.3	22.4	35.9
Ce	24.3	18.7	21.5	18.0	50.3	74.9
Nd	9.1	9.5	10.6	9.3	21.3	33.1
Sm	3.3	2.3	2.2	2.3	4.3	5.9
Eu	1.1	0.8	0.6	0.8	0.9	1.5
Gd	3.5	2.6	2.0	2.7	3.9	6.2
Dy	3.2	2.6	1.9	2.6	3.5	4.9
Er	1.7	1.5	1.1	1.4	1.9	2.4
Yb	1.4	1.4	1.1	1.4	1.8	2.1

Table 3.Isotopic compositions of representative Setouchi volcanic rocks, terrigenous sediments and pelagic sediments.

Location	Sample	rock type	$^{206}Pb/^{204}Pb$	2σm	$^{207}Pb/^{204}Pb$	2σm	$^{208}Pb/^{204}Pb$	2σm
Shodo-Shima								
	SDSYB	basalt	18.314	2	15.562	2	38.468	6
	SD-261	HMA	18.371	2	15.584	2	38.573	5
	SD407	HMA	18.361	9	15.571	9	38.551	20
	SD411	HMA	18.367	3	15.580	3	38.566	5
	SD812	HMA	18.365	5	15.582	2	38.591	6
	MDYB-2	HMA	18.370	3	15.582	3	38.547	6
	UDY	andesite	18.362	1	15.584	1	38.568	3
	SDWHJ	andesite	18.325	3	15.555	2	38.466	5
	SD515	andesite	18.359	5	15.573	5	38.544	9
Takamatsu								
	TK101	basalt	18.315	2	15.567	2	38.503	6
	SH7201	HMA	18.391	2	15.594	2	38.651	4
	JA-2	HMA	18.394	2	15.598	2	38.668	4
	TK6`	andesite	18.414	4	15.608	4	38.718	10
	TK-KAN	andesite	18.402	3	15.596	2	38.670	6
Osaka								
	TGI-5	HMA	18.453	2	15.596	1	38.679	4
	TGI-6	HMA	18.444	1	15.584	1	38.624	4
	NBY-5	HMA	18.425	3	15.586	4	38.629	7
	SG-2	HMA	18.461	2	15.594	2	38.656	5
	NJSB	HMA	18.431	2	15.592	2	38.638	6
	NJIB	HMA	18.438	2	15.593	3	38.648	5
Nankai Trough Site 582, DSDP Leg 87								
	T-1	turbidite	18.503	3	15.614	3	38.755	7
	T-3	turbidite	18.530	5	15.626	5	38.804	9
	T-4	turbidite	18.463	5	15.599	5	38.683	10
	T-6	turbidite	18.509	2	15.619	2	38.763	4
	T-8	turbidite	18.458	3	15.589	4	38.682	12
	T-9	turbidite	18.490	2	15.619	2	38.767	4
	T-10	turbidite	18.500	2	15.609	3	38.752	8
	T-COM	turbidite	18.510	3	15.620	3	38.761	7

Table 3. (continued)

Location	Sample	rock type	$^{206}Pb/^{204}Pb$	2σm	$^{207}Pb/^{204}Pb$	2σm	$^{208}Pb/^{204}Pb$	2σm
Philippine Sea	GDP15-12							
	P-1	pelagic clay	18.625	2	15.629	2	38.827	5
	P-6	pelagic clay	18.605	3	15.627	3	38.790	7
	P-12	pelagic clay	18.683	2	15.644	1	38.889	4
	P-COM	pelagic clay	18.666	2	15.648	2	38.887	6
Nabari, Nara Prefecture								
	NBN-1	gneiss	18.554	1	15.611	2	38.700	3
	SR-1	gneissose gr.	18.526	2	15.624	2	38.712	5
	SR-2	gneissose gr.	19.298	2	15.670	2	39.786	6
	NBR2-3	granite	18.502	2	15.626	2	38.742	6
Uta-Shima, Yamaguchi Prefecture								
	U-X	granulite (xenolith)	18.461	2	15.574	2	38.446	6

Table 3. (continued)

Location	Sample	$^{87}Sr/^{86}Sr$	2σm	$^{87}Sr/^{86}Sr(14Ma)$✣	$^{143}Nd/^{144}Nd$	2σm	εNd
Shodo-Shima							
	SDSYB*	0.70446		0.70439	0.512747		2.1
	SD-261*	0.70512		0.70490	0.512700		1.2
	SD407*	0.70522		0.70502	0.512723		1.7
	SD411*	0.70518		0.70491	0.512717		1.5
	MDYB-2*	0.70510		0.70487	0.512731		1.8
	UDY*	0.70539		0.70516	0.512645		0.1
	SDWHJ	0.704935	14	0.70477	0.512586	16	-1.0
Takamatsu							
	TK101*	0.70413		0.70408	0.512830		3.7
	SH7201	0.706104	25	0.70596	0.512502	20	-2.7
	JA-2	0.70637#		0.70621	0.512550†		-1.7
	TK6`	0.706820	18	0.70656	0.512506	17	-2.6
	TK-KAN	0.706721	17	0.70649	0.512455	19	-3.6
Osaka							
	TGI-5*	0.70524		0.70514	0.512588		-1.0
	TGI-6	0.705154	18	0.70507	0.512562	19	-1.5
	NBY-5*	0.705460		0.70537	0.512553		-1.7
	SG-2*	0.704740		0.70468	0.512734		1.9
Nankai Trough Site 582, DSDP Leg 87							
	T-COM	0.708647	19	0.70829	0.512383	14	-5.0
Philippine Sea GDP15-12							
	P-COM	0.712118	19	0.71173	0.512325	16	-6.1
Nabari, Nara Prefecture							
	NBN-1	0.709828	18	0.70964	0.512386	20	-4.9
	SR-1	0.707508	19	0.70729	0.512313	13	-6.3
	SR-2						
	NBR2-3	0.709271	22	0.70914	0.512195	28	-8.6
Uta-Shima, Yamaguchi Prefecture							
	U-X	0.704806	19		0.512599	12	-0.8

* Data from Ishizaka and Carlson (1983).

✣ Age corrected for 14 Ma

Data from Ando and Shibata (1988)

† Data from Arakawa (1992)

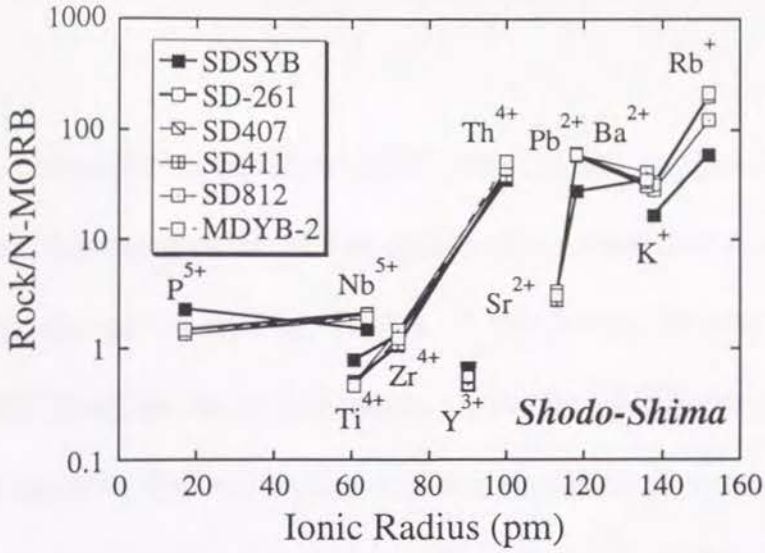

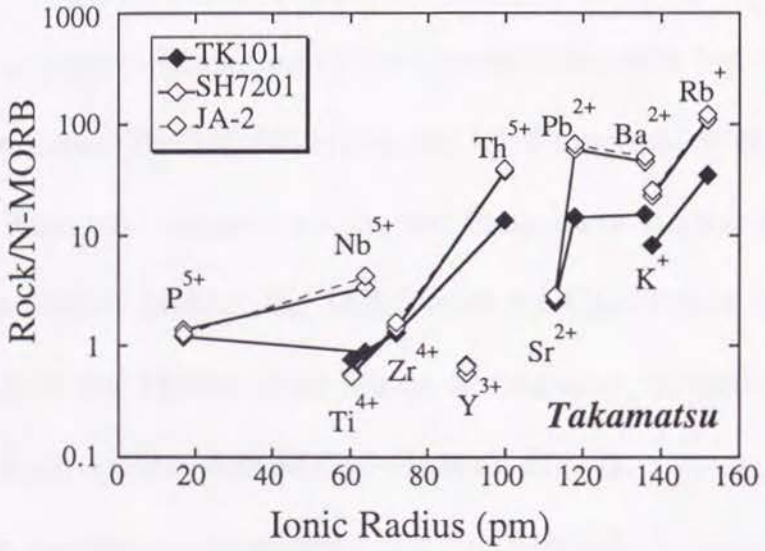

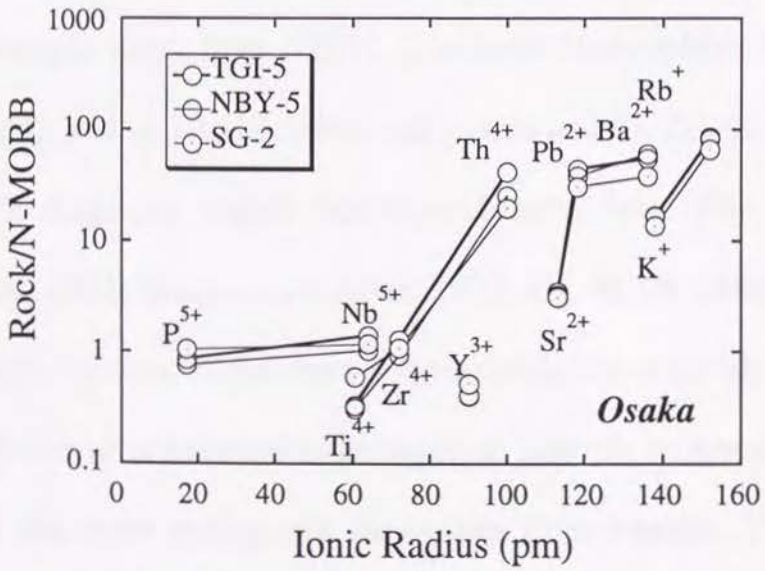

Fig.6. N-MORB-normalized trace element concentrations of the Setouchi volcanic rocks. Solid symbols are basalts and open symbols are HMAs. Values of N-type MORB are taken from Sun and McDonough (1989).

CI-chondrite normalized-REE patterns for representative Setouchi rocks and the composite of the terrigenous sediments and the pelagic sediments are given in Fig. 7. All of the Setouchi samples have high LREE/HREE ratios. Both sediments show the LREE enrichment, general characteristics of the sediments and the continental crustal material. The average compositions of pelagic sediments have higher LREE contents than the average composition of terrigenous sediments, but they have similar HREE contents. Further, the sediments have much more enriched in LREE than the Setouchi volcanic rocks, but these have similar HREE contents. Among primitive HMAs, the TGI-5 from the Osaka area, has lower HREE content than the SD261 from Shodo-Shima area, nevertheless TGI-5 has higher LREE content than SD261 (Table2, Fig. 7).

Pb isotopic compositions for the Setouchi volcanic rocks clearly form a steeper array than NHRL (Northern Hemisphere Reference Line; Hart, 1984), and situated between sediments and the Japan Sea floor basalts on Pb-Pb diagrams (Japan Sea floor basalts data from Tatsumoto and Nakamura, 1991; Cousens and Allan, 1992; Fig. 8). Pb isotopic compositions of Setouchi volcanic rocks show a remarkable linear trend; HMAs from the Shodo-Shima area have the most depleted isotopic compositions, similar to those of the most radiogenic Japan Sea floor basalts. The HMAs from Osaka area have the most enriched Pb isotopic compositions, which overlap some terrigenous sediments on Pb-Pb diagrams (Fig. 8). HMAs in Takamatsu area are situated between Shodo-Shima HMAs and Osaka HMAs on Pb-Pb

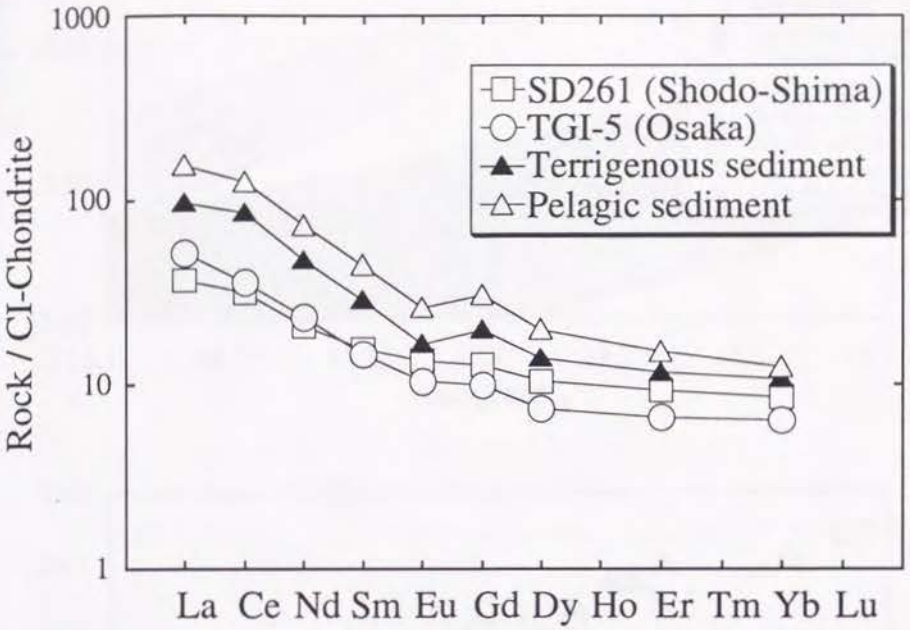

Fig. 7. CI-chondrite normalized REE patterns of the pelagic sediment, terrigenous sediment and the representative HMAs from Shodo-Shima and Osaka areas.

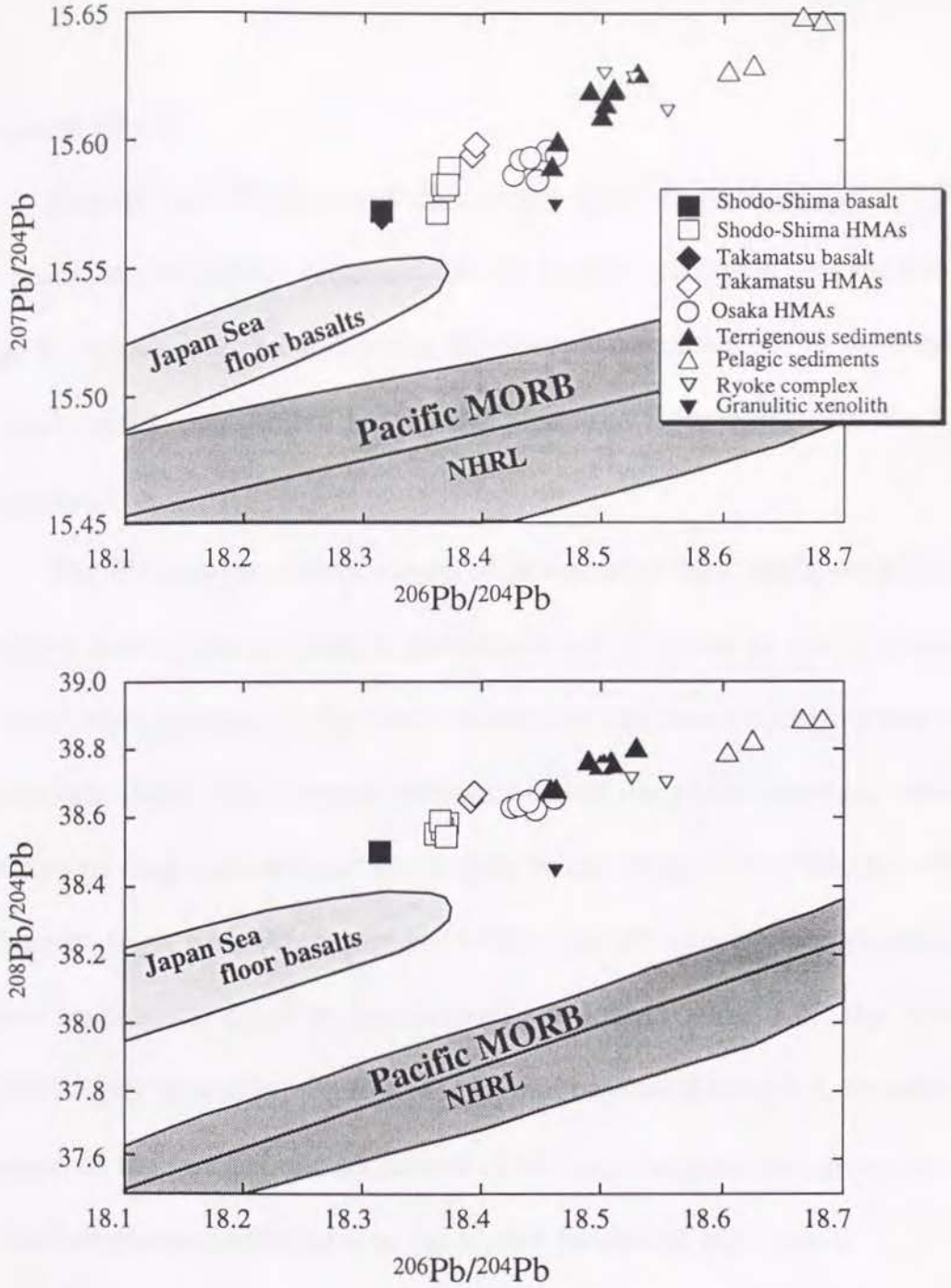

Fig.8. Pb isotopic ratios of the Setouchi volcanic rocks, terrigenous sediments, pelagic sediments, Ryoke basement rocks, granulitic xenolith, Japan Sea floor basalts and Pacific MORBs. NHRL is also shown (Hart, 1984). Data of Japan Sea floor basalts are taken from Tatsumoto and Nakamura (1991) and Cousens and Allan (1992). Values of Pacific MORBs are taken from White et al. (1987) and Cohen and O'Nions (1982).

diagrams (Fig.8).

Basalts and HMAs have distinctive isotopic compositions; HMAs are higher, consequently sediment-like Pb isotopic compositions than basalts (Fig. 8). Basalts have most depleted Pb isotopic compositions of the Setouchi volcanic rocks, i.e., plotted nearby the Japan sea floor basalts on the Pb-Pb diagrams.

The Pb isotopic compositions of terrigenous sediments are relatively depleted than those of pelagic sediments and overlap to the reported Pb isotopic compositions of the shales from the Shimanto belt (Ishikawa and Nakamura, 1994). The isotopic compositions of the present pelagic sediment samples plotted well within the compositional range of the Pacific pelagic sediments (e.g., Ben Othman et al., 1989). The Pb isotopic compositions of upper continental crust in the Setouchi volcanic zone, i.e., the granite, gneissose granite and gneiss from the Ryoke basement complex, are identical to those of the terrigenous sediments. This may suggest that provenanence of the terrigenous sediment was the Ryoke basement complex.

The Nd-Sr isotopic compositions of the Setouchi volcanic rocks exhibit an overall negative correlation within the "mantle array" (Fig. 9), but this trend is less obvious than Pb-Pb diagrams. The Setouchi volcanic rocks are also plotted between sediments, especially the terrigenous sediment, and Japan Sea floor basalts. Basalts and HMAs are also in separated fields, and the latter have also enriched $^{87}Sr/^{86}Sr$ and $^{143}Nd/^{144}Nd$ ratios than the former (Ishizaka and Carlson, 1983).

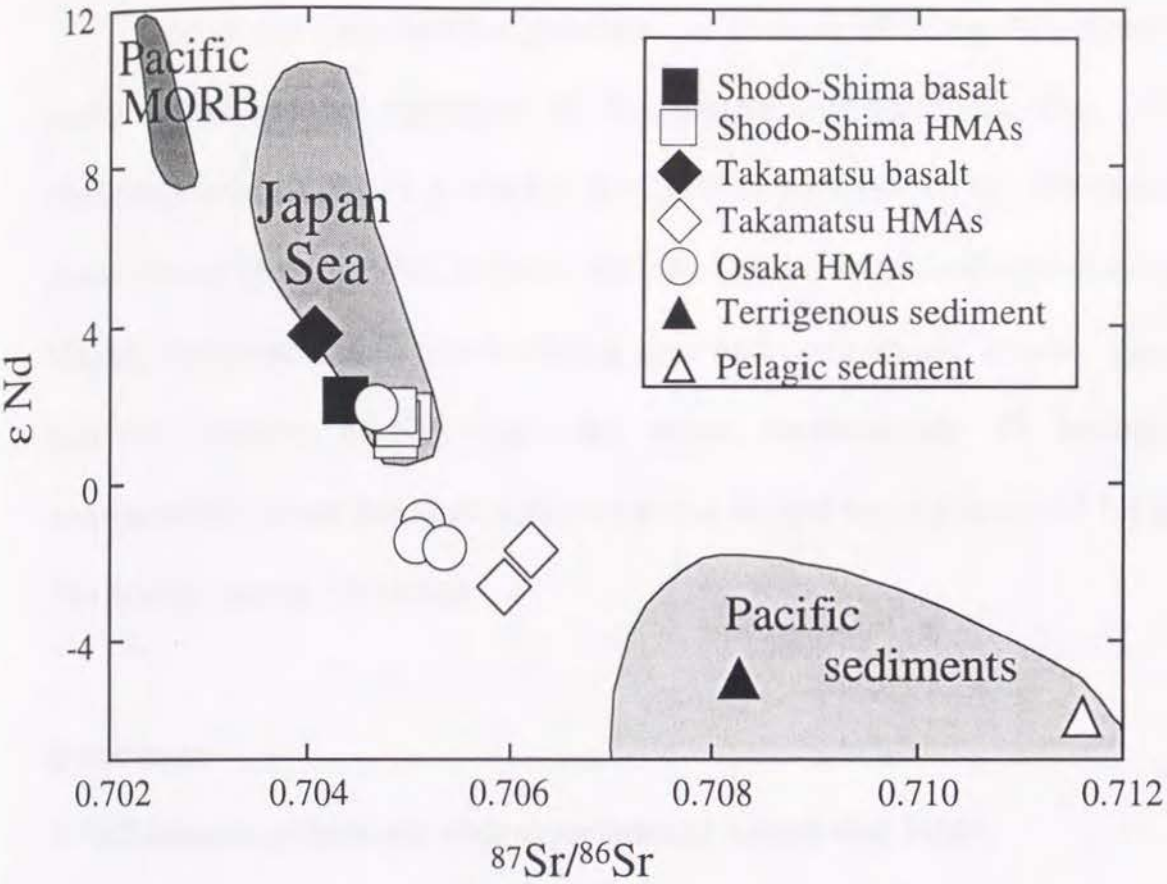

Fig. 9. Nd and Sr isotope ratios of the Setouchi volcanic rocks, Pacific MORB, Japan sea floor basalts, terrigenous sediment, pelagic sediment and Pacific sediment. Data of Pacific MORBs are taken from White et al. (1987) and Cohen and O'Nions (1982). Values of Japan Sea floor basalts are taken from Tatsumoto and Nakamura (1991), Cousens and Allan (1992) and Nohda et al. (1992). Isotopic ratios of Pacific sediment are taken from Ben Othman et al. (1989).

One of the most notable geochemical features of Setouchi volcanic rocks is the secular variations of Pb isotopic compositions (Fig. 10). Paleomagnetic studies (e.g. Otofuji et al., 1985; Ishikawa et. al., 1996) and K-Ar dating (Anno, 1995) indicate that the Setouchi volcanic activities in Osaka, Takamatsu, and Shodo-Shima area had commenced at pre-, syn-, and post-rotation of SW Japan arc sliver, respectively. Pb isotopic compositions of the Setouchi volcanic rocks shifted toward those of Japan Sea BABB during 15-14 Ma.

Discussion

1. Differences of isotopic characteristics of basalt and HMA

Pb isotopic compositions of HMAs are systematically different from those of basalts as well as the Nd-Sr system (Ishizaka and Carlson, 1983; Fig. 8, 9). Mechanisms responsible for these isotopic differences between basalts and HMAs are examined in terms of (1) crustal contamination, (2) mantle heterogeneity, (3) incorporation of SDSC. In order to evaluate the dominant process, a pair of the Shodo-Shima basalt and HMA was chosen, because those erupted simultaneously at the same region, suggesting that spatial and temporal heterogeneity within the mantle source would be negligible.

Crustal contamination

Unfractionated characteristics both for basalt and the HMA, which

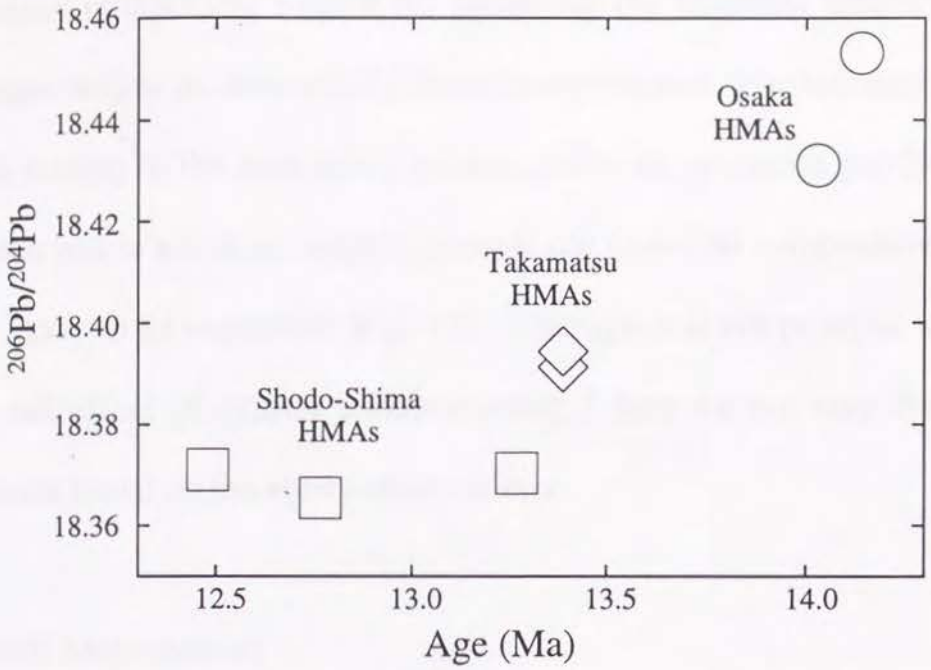

Fig. 10. Through-time variation of Pb isotopic compositions of the Setouchi HMAs

were deduced by petrographical, chemical and melting phase relation studies (e.g., Tatsumi and Ishizaka, 1981, 1982a, 1982b; Tatsumi 1982), may provide a rather compelling reason for believing the minimal effect of crustal contamination in determining those compositions. Furthermore, even the bulk mixing of the underlying granite, gneiss or gneissose granite from the Ryoke belt is assumed, neither isotopic nor chemical composition of HMA are likely to be explained (Fig. 11). Although it is not possible to evaluate the net effect of crustal contamination, I here do not take its role into account based on the above observations.

Mantle heterogeneity

Based on Nd-Sr isotopic compositions of the Setouchi volcanic rocks, Ishizaka and Carlson (1983) inferred that the mantle wedge beneath the SW Japan are chemically stratified and proposed the mechanism of the production of two distinct magmas including that the primary basaltic magmas, generated by partial melting of the variably metasomatized mantle wedge overlying the subducted plate, ascended into the hydrous uppermost mantle characterized by an enriched isotopic signature. Heat from the basaltic magma causes secondary partial melting of hydrous peridotites to produce primary HMA magmas. However this mechanism would be rather *adohoc*, and could not explain the origin of such chemical stratification.

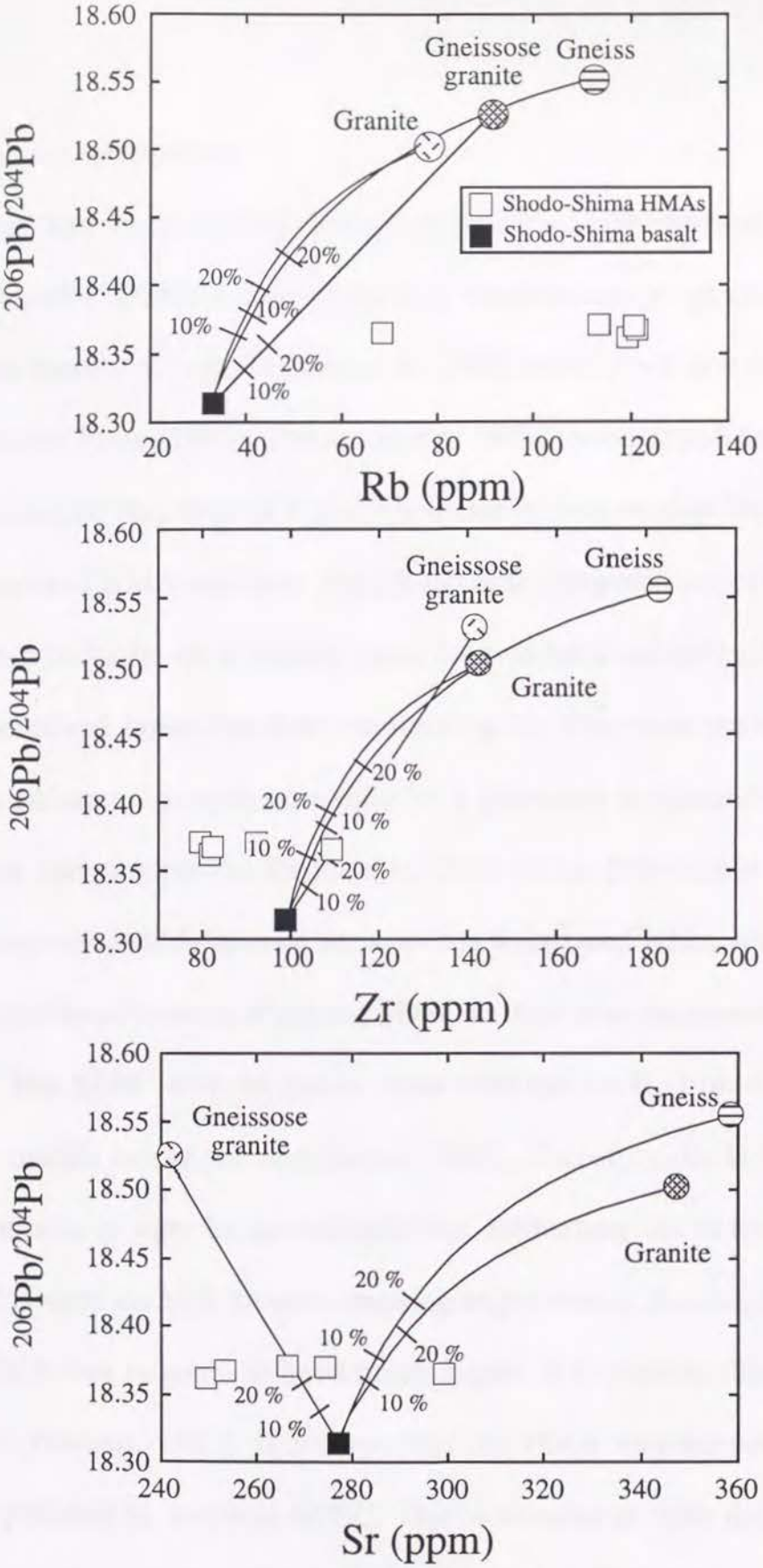

Fig. 11. Three hypothetical mixing lines between Shodo-Shima basalt and representative crustal materials from basement Ryoke complex. Numbers adjacent ticks on mixing curves are the present crustal material in the mixture.

Subduction components

It has been widely accepted that the slab-derived subduction component (SDSC) is one of the key components in governing the arc magma chemistry (e.g., Tatsumi et al., 1986; McCulloch and Gamble 1991; Pearce and Peate, 1995). The amount of SDSC overprinted on the original mantle source may thus be a possible factor in determining the composition of basalt and HMA magmas. The Pb isotopic compositions of the Setouchi volcanic rocks lie on a mixing trend formed between pelagic/terrigenous sediments and Japan Sea floor basalts (Fig. 8). Therefore the incorporation of the sediment component would be a plausible mechanism to produce isotopic variations of the Setouchi volcanic rocks. This would indicate that the compositional difference between the basalt and HMA may be caused by the different amount of adding SDSC in their magma source.

The SDSC may be much more enriched in H_2O than the original upper mantle before the addition of SDSC. Therefore the H_2O content of magma source may be an indicator for estimating the amount of added SDSC. Based on high pressure melting experiments, the magma source of the HMA was inferred to have much higher H_2O content than that of the basalt (Tatsumi, 1982). It follows that the HMA magma source may be more polluted by hydrous SDSC. This is consistent with the Pb isotopic variations, because the SDSC would have higher Pb isotopic compositions than arc magmas (e.g., Ben Othman et al., 1989; Ishikawa and Nakamura, 1994).

Nd-Sr isotopic compositions exhibit a mixing trend unclearer than the trend for Pb isotopes. This may be attributed to widely spread Nd-Sr isotopic compositions of SDSC than the Pb isotopes (Fig. 12). The differences of Pb, Nd and Sr concentrations between the sediments and the altered MORB inferred to be about a hundred-fold, fore-fold and nearly identical, respectively. Since the ratio of the altered MORB and sediment in SDSC would not be constant in each areas, the Nd and Sr isotopic compositions of SDSC are more highly varied than Pb isotopic compositions (Fig. 12), and thus precluded to form mixing line.

2. Metasomatic agent

One of the highly controversial problems in geochemistry is whether the SDSC is melt or H_2O fluid. The elemental ratios of HFSE could provide a key constraint for this problem, because HFSE are strongly partitioned into a partial melt as an incompatible element but not into an aqueous fluid. The HMAs have higher Nb/TiO_2 and Zr/TiO_2 ratios and lower TiO_2 concentraions than the basalts, namely, these are clearly separated fields on TiO_2 variation diagrams for Zr/TiO_2 and Nb/TiO_2 (Fig. 13). Among HFSE, distribution coefficient of TiO_2 would be higher than those of other HFSE (e.g., McCulloch and Gamble, 1991; Stolper and Newman, 1994). Since basalts and HMAs erupted simultaneously in the small area, it is reasonable to assume that the original mantle compositions for these two magma types are identical. This means that TiO_2 concentrations will positively correlate

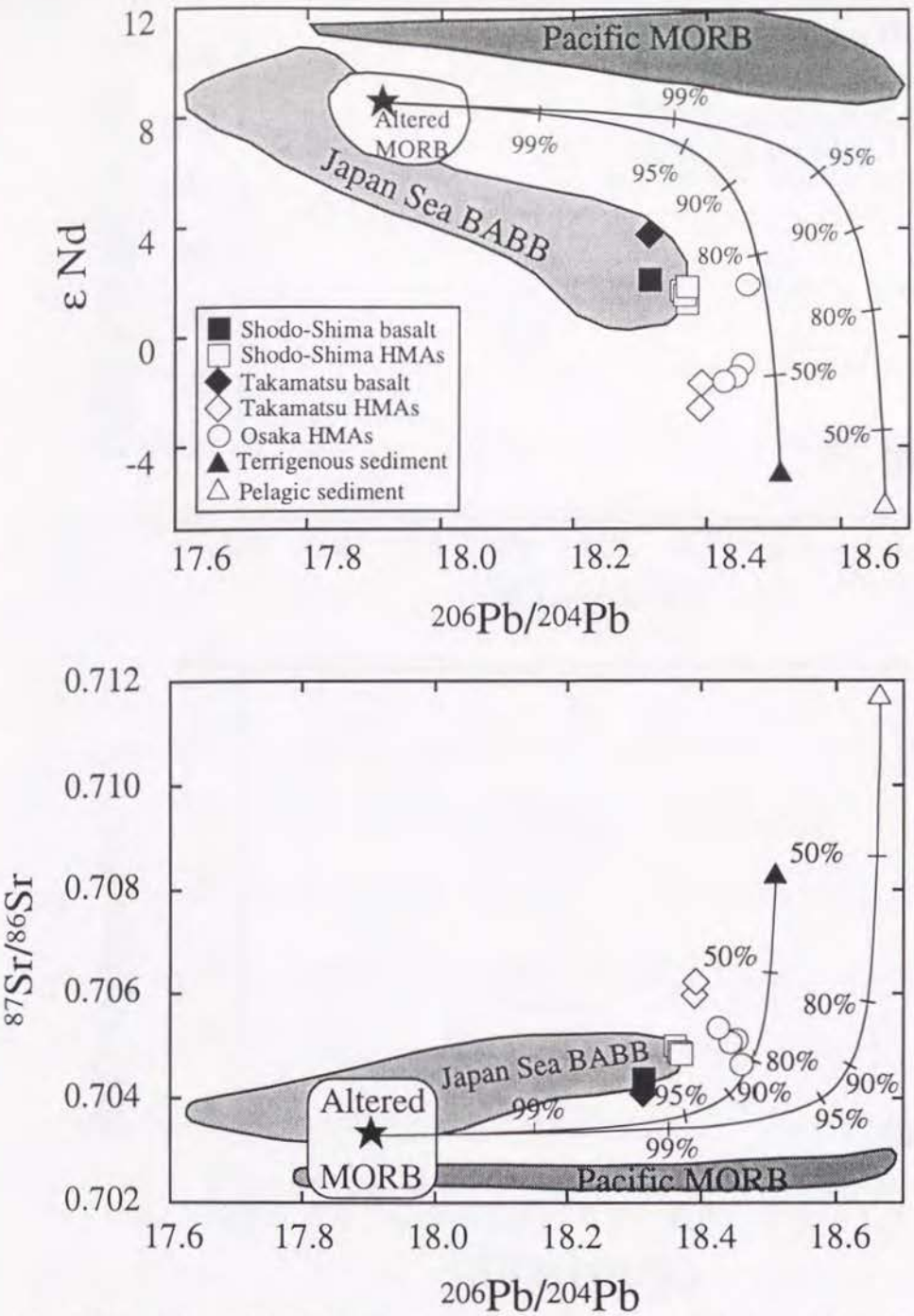

Fig. 12. Two hypothetical mixing lines between altered MORB and, terrigenous and pelagic sediments. Pb and Nd isotopic ratios of altered MORB are assumed to be identical to those of Shikoku basin Sea floor basalts (data from Hickey-Vargas, 1991). The values used to mixing calculations were averages of these basalts, i.e., $^{206}Pb/^{204}Pb$ = 17.904 and ε Nd = 8.6. Sr isotopic ratios of altered MORB are assumed to be identical to those of unleached Mariana Trough basalts (data from Stern et al., 1990). Thus average ratio of these basalts, i.e., $^{87}Sr/^{86}Sr$ = 0.70326, were used to mixing calculation. Pb, Nd and Sr concentrations of altered MORB are 0.3, 7.3 and 110 ppm, respectively (data from McCulloch and Gamble, 1991). Representatives of subducted terrigenous and pelagic sediments are auumed to be identical to T-COM and P-COM, respectively which are composite samples of sediments analyzed in this study. Numbers adjacent ticks on mixing curves are the present altered MORB component in the mixture.

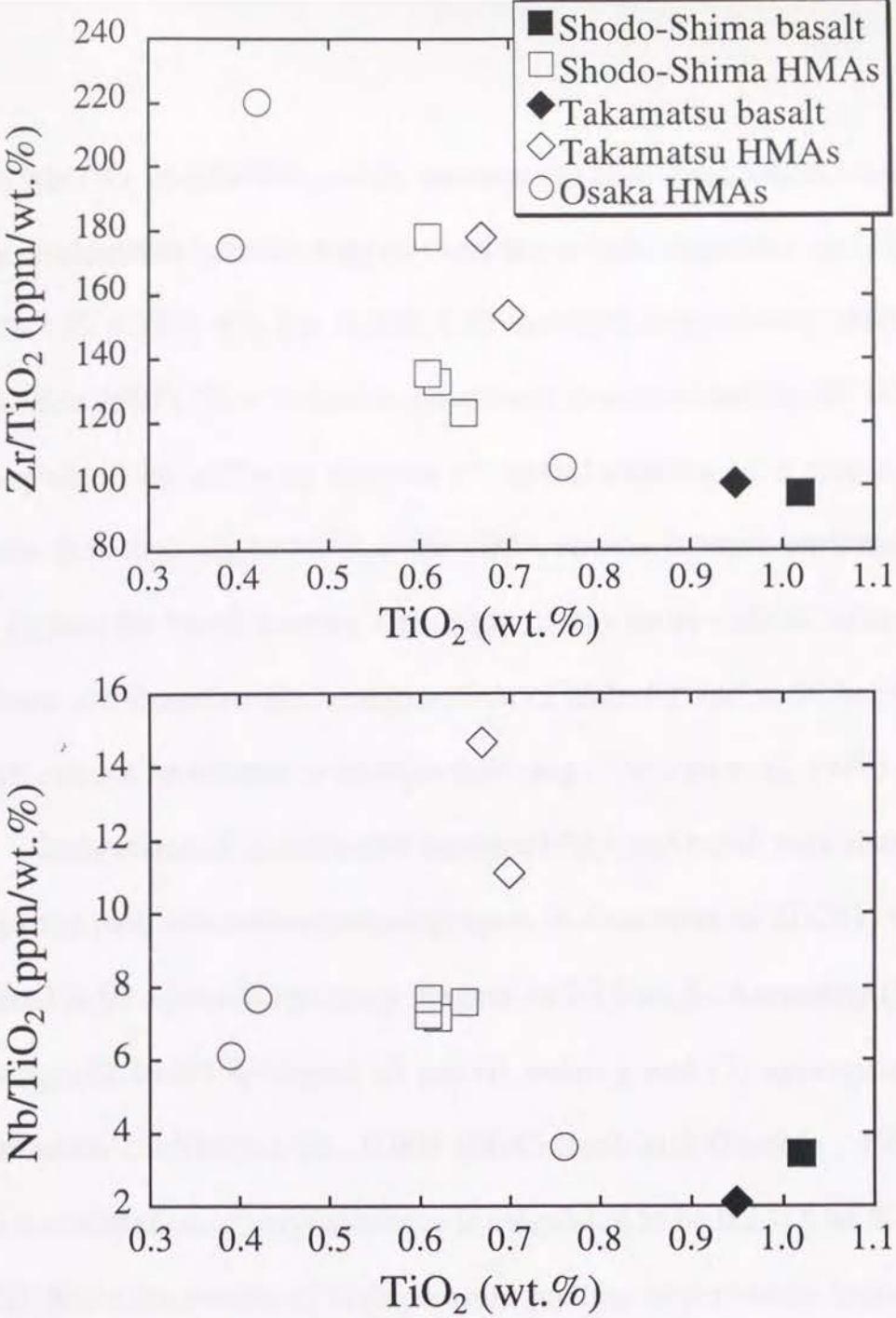

Fig.13. TiO_2-HFSE/TiO_2 ratios diagrams for the Setouchi HMAs and basalts.

with Nb/TiO_2 and Zr/TiO_2 ratios, because the bulk distribution coefficients of these elements between magmas and the mantle peridotite are inferred to be $Nb < Zr < TiO_2 < 1$, i.e., 0.008, 0.05 and 0.07, respectively (McCulloch & Gamble 1991). Therefore, the constraints observed among HFSE cannot be explained by differing degrees of partial melting of a single mantle source. It is thus suggested that the HMA source is more enriched in Nb and Zr than the basalt source. The origin of this source characteristics may be better attributed to the metasomatism of slab-derived melt, because the HFSE can not be soluble in an H_2O-fluid (e.g., Tatsumi et al, 1986).

Comparison of K_2O content between HMA and basalt may also support the partial melt as a metasomatizing agent. K_2O content of SD261, which is inferred to be a possible primary magma, is 2.25 wt.%. Assuming (1) batch melting, (2) 10-20 % degree of partial melting and (3) appropriate bulk distribution coefficient, i.e., 0.004 (McCulloch and Gamble , 1991), the K_2O concentration of magma source is calculated to be 0.2-0.5 wt.% (Shaw, 1970). Since the results of high pressure melting experiments indicate that the HMA magma contains 7 wt.% H_2O (Tatsumi, 1982), the H_2O content in magma source would be 0.7 to 1.4 wt.%. Further, the upper limit of H_2O concentration in magma source would be 1.5 to 3.0 wt.%, because the H_2O solbility in HMA magmas were inferred to be 15 wt.% at 1.5 GPa (Tatsumi, 1981). Assuming that the SDSC is aqueous fluid and the original mantle compositions are identical to Japan Sea BABB (Back Arc Basin Basalt) source with 0.0036 wt.% K_2O (Yamasita and Tatsumi, 1994), the addition

of 0.7-3.0 wt.% SDSC must elevate the K_2O concentration from 0.0036 wt.% to 0.2-0.5 wt.%. This means that the K_2O concentration in the SDSC would be 15-33 wt.% (Fig. 14). The distribution coefficients between fluid and peridotite are hundred times higher than those between melt and peridotite (Hawkesworth et al., 1993). Moreover, the distribution coefficients between fluid and slab may be much higher, because there may be K-bearing phases. It is thus suggested that such a high concentrations, i.e., about ten times higher than arc magmas which would be representative melt of K enriched mantle, are not realistic for aqueous fluids.

The melt of oceanic crust and sediments, on the other hand, would be felsic (e.g., Nicholls and Ringwood, 1973; Ringwood, 1974; Whilly and Sekine, 1982) and may be saturated in H_2O. Further, the solubility of H_2O in magmas mainly depend on pressure. Here, considering that the H_2O solubility in andesitic melt had been reported to be 10 wt.% at 1.5 GPa (Sakuyama and Kushiro, 1979), the H_2O concentrations of SDSC may be about 10 wt.%. It follows that the amount of SDSC in magmas source would be 7-14 and 15-30 wt.% at the case of HMAs magmas undersaturated H_2O and saturated H_2O, respectively. To elevate the K_2O content from 0.0036 wt.% to 0.2-0.5 wt.% by the addition of 7-30 wt.% SDSC, the K_2O concentration of SDSC would be 1.5-3.3 wt.% (Fig. 14). If the major component of the SDSC generated by the melting of the sediment layer, this value may be acceptable, because these values are in the range of natural metasediments (e.g., Table 1; Yuhara, 1994) and the results of

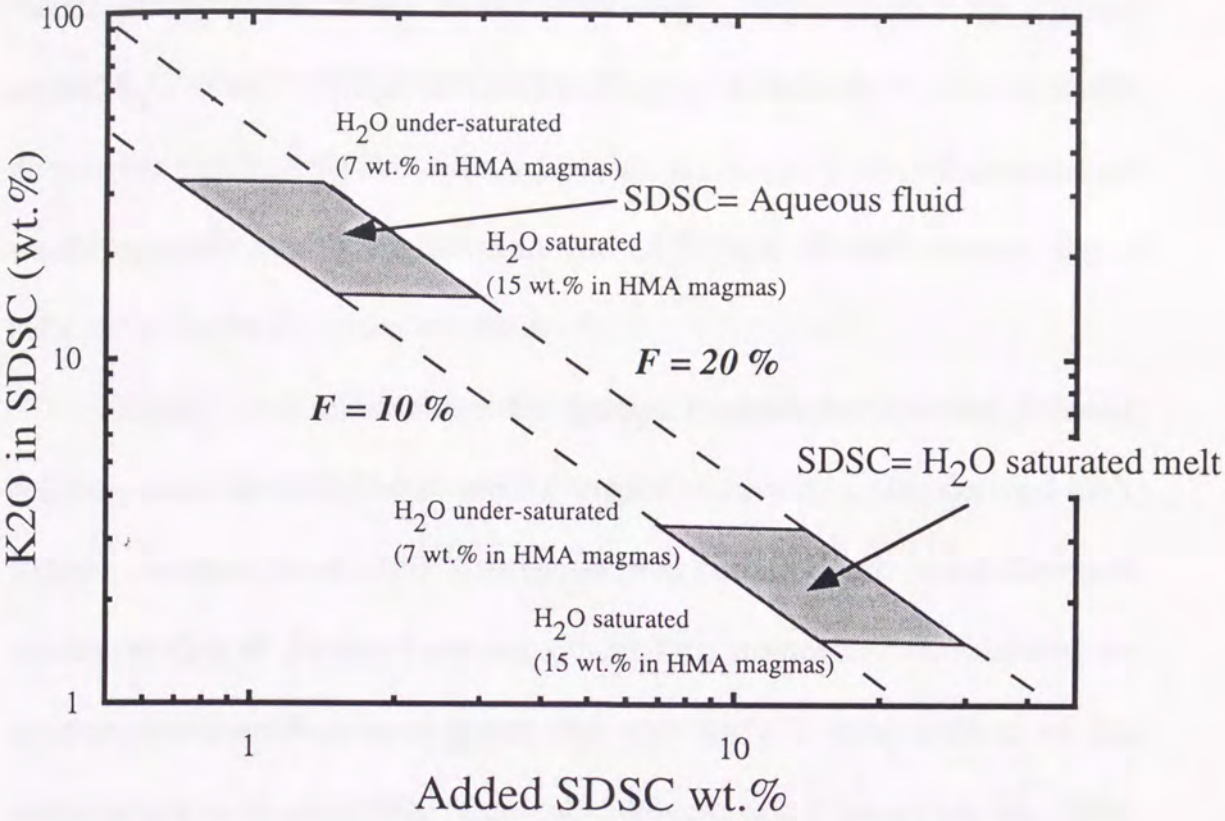

Fig. 14. Amount of added SDSC-SDSC K_2O concentration diagaram. K_2O concentration of SDSC is calculated based on following four constraints: (1) original mantle compositon is assumed to be identical to Japan Sea BABB source with 0.0036 wt.% K_2O (Yamashita and Tatsumi, 1994), (2) all H_2O in magma source is derived from SDSC and is partitioned into magma, (3) H_2O in HMA magmas are in the range between 7-15 wt. % (Tatsumi, 1982), (4) K_2O concentrations of HMA magma sources are calculated by non-modal batch melting with degrees of partial melting (F) between 10-20 %.

melting experiments in pelitic systems (e.g., Vielzeuf and Holloway, 1988; Douce and Johnston, 1990; Douce and Beard, 1995). Even if the original mantle K_2O composition is identical to N-type MORB source, above results do not alter significantly, because K_2O concentration of HMA magma sources would be considerably higher than that of N-type MORB source, that is believed to be on the order of 0.01 wt.%.

Estimation of temperature distribution beneath the Setouchi volcanic belt may also advocate the element transportation with a slab derived melt. Using a constraint that 1100 °C is required at certain depth in sub-Setouchi mantle wedge at depths between 60-30 km, numerical simulations on temperature distribution suggest that the surface temperature of the subducting slab is about 900 °C at sub-Setouchi belt (Tatsumi et al., 1996; Furukawa and Tatsumi 1996). The solidus temperature of peritic system at sub-Setouchi, i.e., at 1.5 GPa, would be about 800 and 700 °C under H_2O-absent and present condition, respectively. It follows that the pelitic rocks in downgoing slab would melt beneath the Setouchi region. Furthermore, DSDP drilling had shown that the off-ridge volcanism occurred in the Shikoku Basin around 15 Ma (Klein et al., 1978; Klein and Kobayashi, 1980) and this suggests that the subducted plate was still hot at the time of Setouchi volcanism. Therefore, the plausible mechanism to pollute mantle wedge is the elements transportation by melt.

3. The nature of SDSC

3-1. Sediment derived component

Nd-Sr isotopic compositions suggest that the major component of SDSC would be sediment derived component, because basalts and HMAs exhibit a negative correlation which would be produced by the addition of SDSC (previous section; Fig. 9). Arc magmas, which are formed by addition of altered MORB derived fluid, characterized by positive correlation on Nd-Sr diagram (e.g., Tatsumi et al., 1991; Tatsumi et al., 1992). Thus the negative trend on Nd-Sr diagram suggest the relatively minor contribution of altered MORB crust derived component, but the major contribution of sediment derived component with high $^{87}Sr/^{86}Sr$ and low $^{143}Nd/^{144}Nd$ ratios.

The Pb concentration of HMA ranges from 11 ppm to 19 ppm, i.e., forty-fold to sixty-fold of that of N-type MORB. The N-type MORB source is believed to be representative of upper mantle. Further, Pb concentrations of N-type MORB source and Japan Sea BABB source are nearly identical, which are inferred to be 0.05 and 0.06 ppm , respectively (e.g., Ben Otheman et al., 1989, for N-type MORB source; Yamashita and Tatsumi, 1994, for Japan Sea BABB source). Therefore, the most of Pb in HMA magma source would be derived from SDSC. This means that among the possible subduction sediments contributing to adding SDSC, the terrigenous sediment may play a more dominant roles, because the fact that some overlap of Osaka HMA and terrigenous sediment on Pb-Pb diagrams strongly suggest that the terrigenous sediment is a dominant component of SDSC (Fig. 8).

3-2. Contribution of altered MORB crust derived component

Based on numerical simulations on temperature distribution in the sub-Setouchi upper mantle, it is suggested that the major component of SDSC would be the sediment derived component (Tatsumi et al., 1996; Furukawa and Tatsumi 1996). However, the following constraints suggest that minor contribution of the SDSC derived from the altered MORB crust must be also indispensable.

Constraints from Pb systems

Pb concentrations of Shodo-Shima HMAs range 17-18 ppm and are about sixty and twenty-sixty times higher than N-type MORB and Japan Sea BABB, respectively. Because the original mantle compositions of the Setouchi volcanic rocks may be identical to N-type MORB source or Japan Sea BABB source, the addition of Pb derived only from the sediments, which can explain Pb concentrations in HMAs, would produce isotopic shifts far larger than those observed, i.e., identical to terrigenous sediment (Fig. 15). Therefore the component, which can shift the Pb isotopic compositions of SDSC to less radiogenic, are required. Possible candidates are altered MORB crust-derived component and the interaction between the mantle and SDSC such as column mantle (e.g., Navon and Stolper 1987). Pb concentrations of the original mantle may be identical to N-type MORB source or Japan Sea BABB source, those are, 0.05 and 0.06 ppm ,

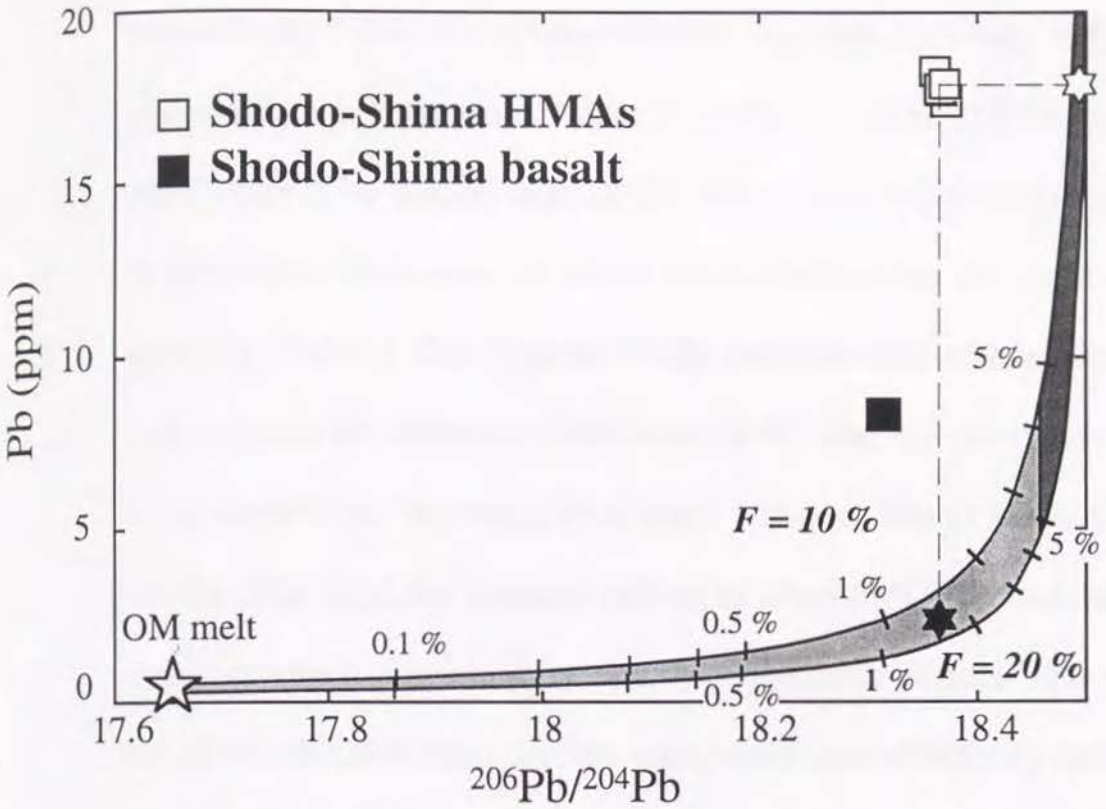

Fig. 15. $^{206}Pb/^{204}Pb$ ratio-Pb concentration diagram for calculated magmas. Shodo-Shima HMAs and basalt are also shown. Isotopic ratios and magma source concentrations of Pb are obtained by bulk mixing calculation of original mantle and terrigenous sediment (T-COM). Original mantle (OM) compositions are assumed to be identical to Japan Sea BABB source with 0.06 ppm Pb(Yamashita and Tatsumi, 1994) and most depleted Japan Sea floor basalt with $^{206}Pb/^{204}Pb$ = 17.645, respectively. Numbers adjacent ticks on curves are the present sediment in the magma sources. Pb concentration of magmas are calculated by non-modal batch melting with 0.015 bulk distribution coeffcient (McCulloch and Gamble, 1991) and degree of partial melt (F) between 10-20%. Hatched area indicate calculated Pb concentration and isotopic ratios of magmas. Dark hatched area denote the isotopic composition ientical to terrigenous sediment. ★and ☆show Pb isotopic and concentration of Shodo-Shima HMAs on calcurated region, respectively.

respectively (data for N-type MORB, e.g., Ben Othman, 1989; data for Japan Sea, Yamashita and Tatsumi, 1994). Those of SDSCs, on the other hand, would be higher than 20-30 ppm, because SDSC would be melt derived from sediments of which Pb concentrations are typically 20-30 ppm (e.g., Table 1; Ben Othman, 1989). Take the difference in concentrations into account, the interaction between SDSC and the mantle wedge seems to be minor factor to change Pb isotopic compositions of SDSC to depleted. On the other hand, the minimal melting of altered MORB crust may produce a melt of which concentration may be on the order of ppm. This means that the altered MORB crust derived component can effectively reduce the Pb isotopic compositions of SDSC relative to interaction between mantle and SDSC. It is thus suggested that the altered MORB crust derived component would be essential in order to dilute SDSC Pb isotopic compositions.

Constraints from the geothermal conditions

The following physical considerations also suggest the possibility of the minimal dehydration melting in the altered MORB crust. Wet solidus of basalt at 1.5 GPa, i.e., depth of slab at sub-Setouchi belt, is inferred about 650 °C (e.g., Green, 1982). Further, the surface temperature of slab is inferred about 900 °C beneath the Setouchi region (Furukawa and Tatsumi, 1996). This may suggest that the temperature of altered MORB crust beneath Setouchi region is well above the wet solidus, because the temperature inside of the downgoing slab, i.e., 5 km below from the surface, is estimated

about 150 °C lower than the top of the slab (Toksöz et al., 1971). Considering that the diminishing of stability field of amphibole would release H_2O continuously (Poli and Schnidt, 1995), the minimal melting of altered MORB crust is plausible.

Further, the age of the subducted Shikoku Basin and the Setouchi volcanism were inferred to be 17-25 Ma and 12-14 Ma respectively (e.g., Kobayashi and Nakamura, 1978; Ishikawa et al., 1996). This would indicate that the age of subducting slab was about 3-13 Ma during the Setouchi volcanism. Based on two-dimensional, heat-transfer model, Peacock (1990) calculated the temperature distribution on the surface of the subducting oceanic crust. The result indicate that the temperature of the top at the oceanic crust with a age of 10 Ma is inferred about 800 °C at the 1.5 GPa, well above the wet solidus, that is 650 °C, but below dry solidus temperature of the altered MORB crust, that is about 1200 °C (e.g., Green, 1982). Considering that the amhibole breakdown at 1.5 GPa is inferred to be about 1100 °C (e.g., Green, 1982), free H_2O in altered MORB crust layer is released only by the diminishing of stability field of amphibole (Poli and Schnidt, 1995). This suggest that the melting of altered MORB crust would occur but the degree of melting probably minimal.

4. Origin of secular variation of Pb isotopic composition

The occurrence of HMAs may be limited to subduction zones where unusually high geothermal gradient is attained. This high geothermal gradient

is attribute both to the young plate subduction and the back arc spreading (e.g., Tatsumi and Maruyama, 1989). It follows that the major heat source of hot mantle wedge is uprising asthenosphere related to the back arc spreading. Supposing that supplied heat may be transmitted by the mass transportation, then the secular variation of Pb isotope compositions would be ascribed to the replacement of source material by the upwelling asthenospheric material (Fig. 16), because the uprising material would have depleted geochemical characteristics (e.g., Yamashita and Tatsumi 1994). Alternatively, two component mixing, namely, single depleted source mantle and SDSC, can also explain the trend on Pb-Pb diagrams, however, the correlation of Pb isotopic compositions and trace element ratios such as Pb/TiO_2 and Pb/Zr are not consistent with this mechanism (Fig. 17).

The trace element ratios would support the compositional change of mantle wedge. The Ba/TiO_2 ratios clearly show the positive correlation with Pb isotopic compositions (Fig. 18), and so are Ba/Y, Ba/Sr and Zr/TiO_2. Based on high pressure melting experiment, it is demonstrated that the total degree of partial melting of the Osaka HMAs were higher than the that of Shodo-Shima HMAs (Tatsumi, 1981, 1982). The bulk distribution coefficients to mantle peridotite are inferred to be Ba < Sr < Zr < Ti < Y, i.e., 0.002, 0.02, 0.05, 0.07 and 0.15, respectively (McCulloch & Gamble, 1991). Therefore, the melt extraction would selectively reduced Ba, Sr and Zr concentrations relative to Ti and Y concentrations in their magma source region. Thus, previous melt extraction strongly reduce Ba/Y, Ba/TiO_2 and

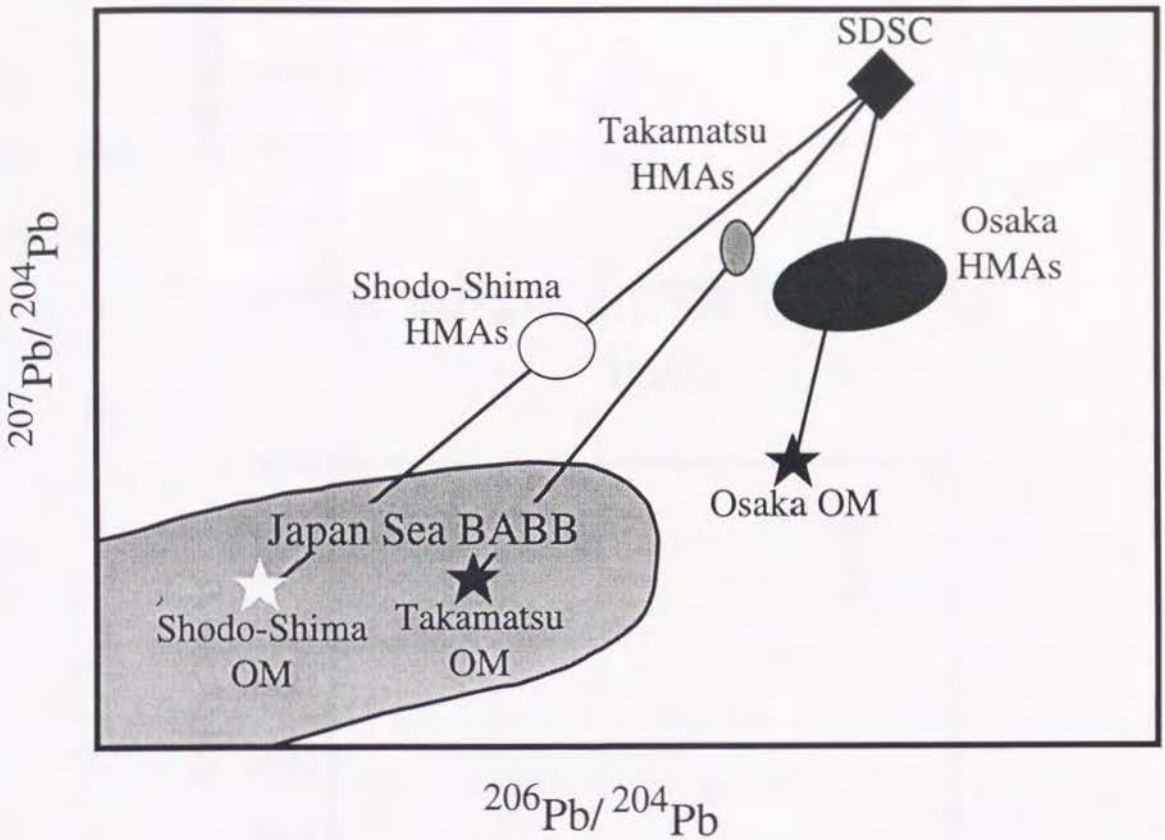

Fig. 16. A schematic Pb-Pb diagram showing a plausible mechanism for producing Pb isotopic variation observed in the Setouchi volcanic rocks. Pb isotopic variation is mainly attributed to compositional chamge of original mantle.

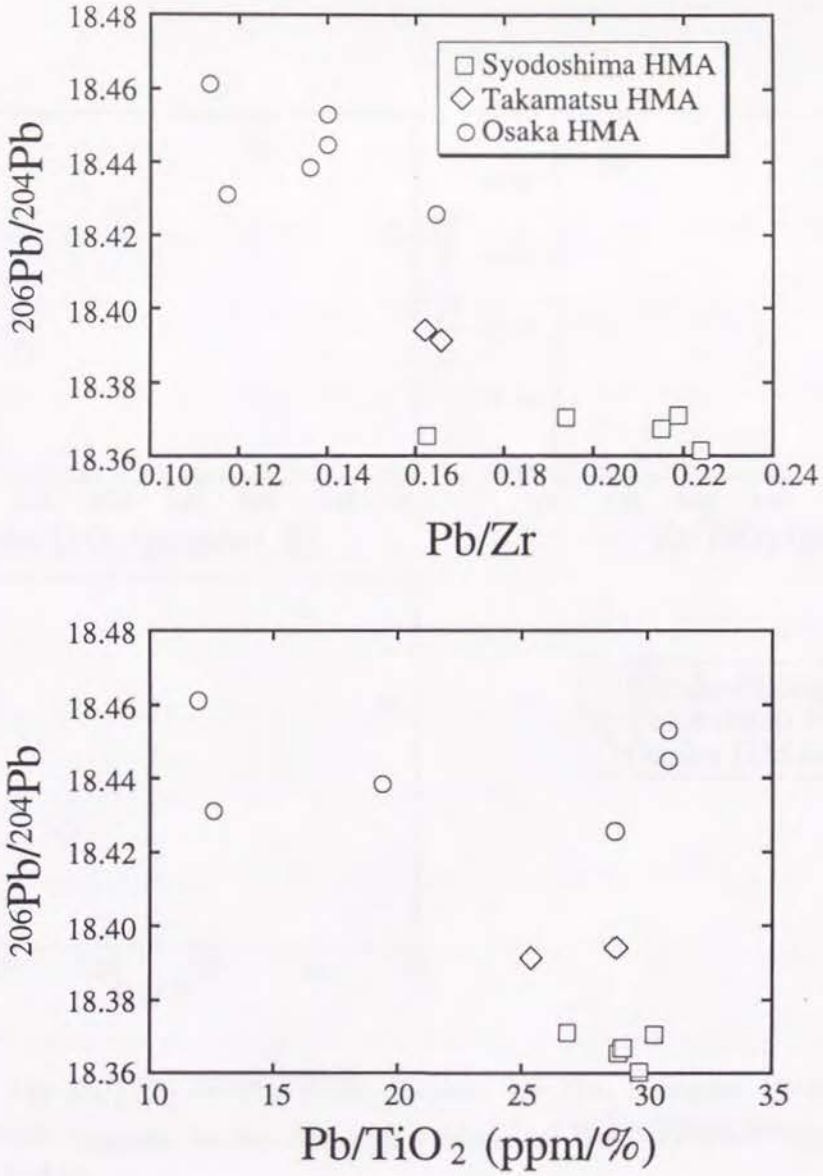

Fig. 17. Pb/Zr-$^{206}Pb/^{204}Pb$ and Pb/TiO_2-$^{206}Pb/^{204}Pb$ diagrams for the Setouchi HMAs.

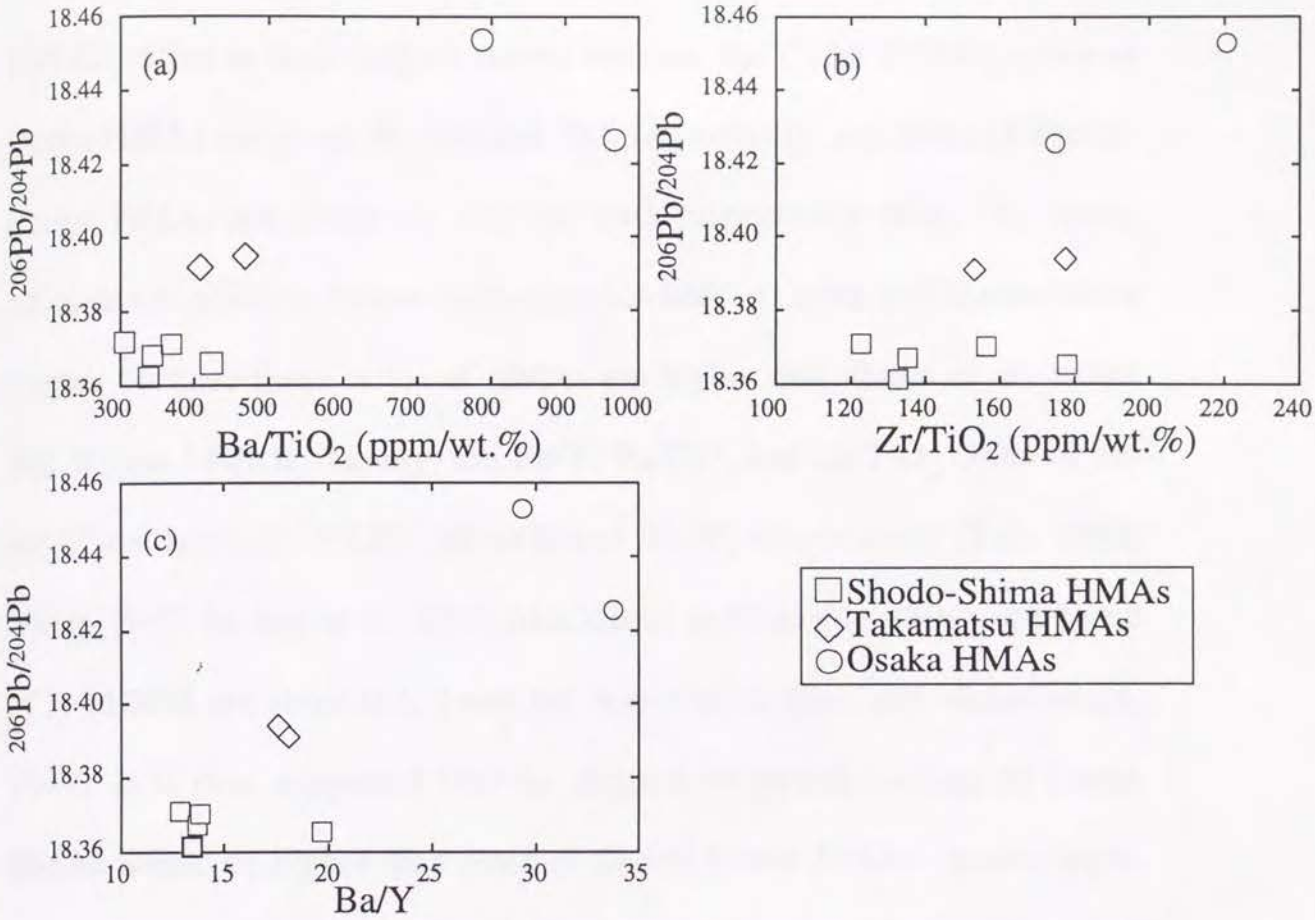

Fig. 18. (a) Ba/TiO_2-$^{206}Pb/^{204}Pb$ diagram for the Setouchi HMAs. (b) Zr/TiO_2-$^{206}Pb/^{204}Pb$ diagram for the Setouchi HMAs. (c) Ba/Y-$^{206}Pb/^{204}Pb$ diagram for the Setouchi HMAs.

Zr/TiO_2 ratios in their magma source regions. Ba/Y and Zr/TiO_2 ratios of Osaka HMAs are about 30, 900 and 200, respectively, and those of Shodo-Shima HMAs are about 14, 350 and 140, respectively (Fig. 18). These ratios would preclude former melt extraction both in Osaka and Shodo-Shima region, because these ratios of HMAs are higher than those of arc basalt and N-type MORB, namely, the Ba/Y, Ba/TiO_2 and Zr/TiO_2 ratios of arc basalt are typically 10-20, 200-400 and 40-80, respectively (Sun, 1980; Ewart, 1982; Hickey et al., 1986; McCulloch and Gamble, 1991), and those of N-MORB are about 0.2, 8 and 60, respectively (Sun and McDonough, 1989). It is thus suggested that the degrees of partial melting of Osaka HMAs would be higher than those of Shodo-Shima HMAs. Accordingly, these trace elemental ratios can not be explained by the different degrees of partial melting and would support the source compositional change. Alternatively, higher elemental ratios indicate that the Osaka magma sources have much SDSCs than the Shodo-Shima magma sources. However, the relative enrichment of the Shodo-Shima HMAs in alkalis over other incompatible elements compare to Osaka HMAs may not be consistent with this mechanism (Fig. 19; Ishizaka and Carlson, 1983), because this geochemical feature suggest that the magma sources of Shodo-Shima HMAs would have much more SDSCs than those of Osaka HMAs.

CI-chondrite normalized REE patterns also advocate the source compositional change (Fig. 7). Osaka HMA has higher LREE and lower HREE concentrations than Shodo-Shima HMA. This suggest that the source

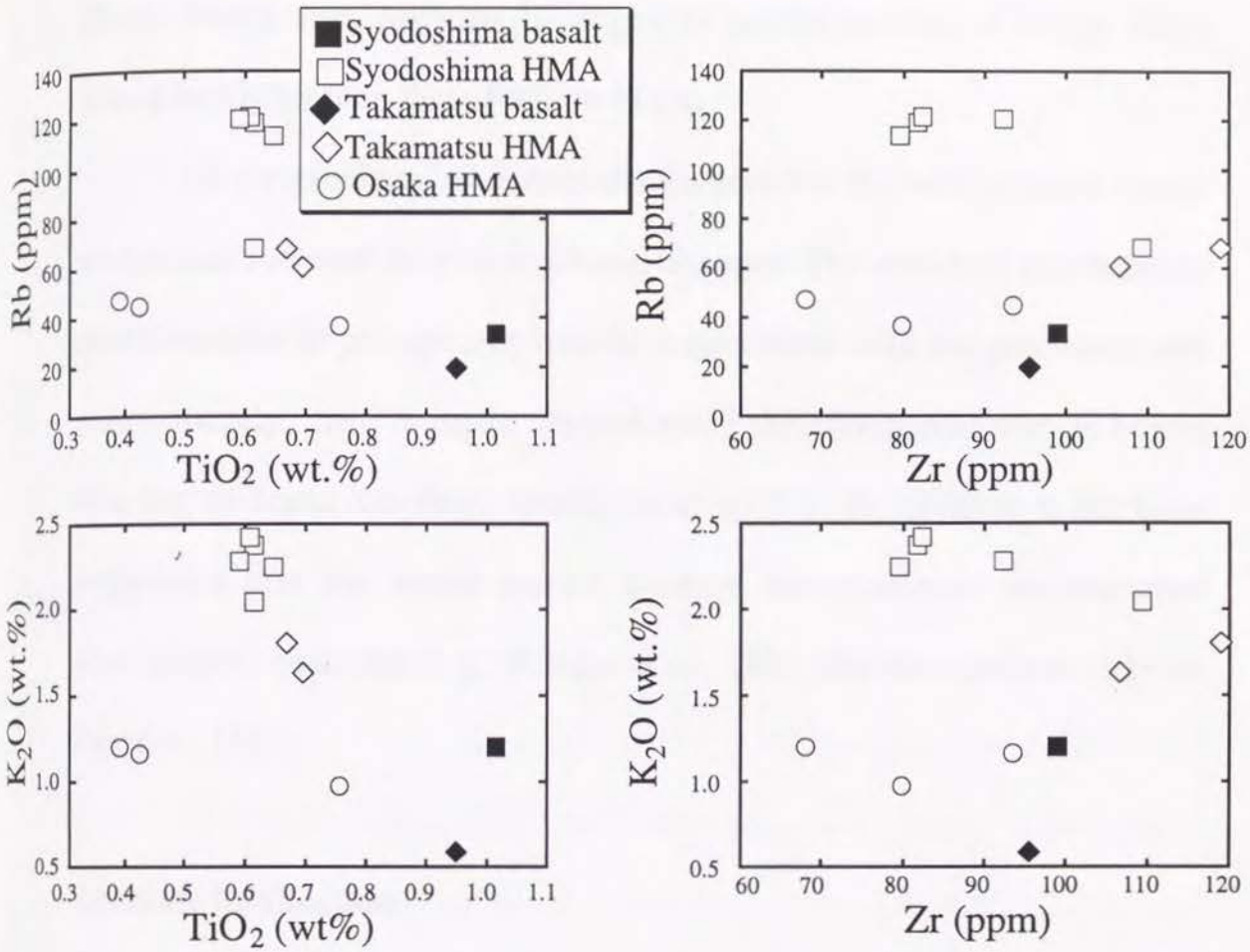

Fig. 19. TiO_2-alkaline metal elements and Zr-alkaline metal elements diagrams for the Setouchi volcanic rocks. Relative enrichements of alkaline metal elements over other imcompatible elements are larger in HMAs from Shodo-Shima than those from Osaka and Takamatsu.

mantle beneath the Osaka area was enriched relative to that beneath the Shodo-Shima area, because the degree of partial melting of Osaka HMA would be higher than that of Shodo-Shima.

Above geochemical constraints suggest that the sub-Setouchi mantle wedge had suffered the compositional changes. The enriched geochemical characteristics of pre-opening mantle is consistent with the paleomagnetic study, namely, the SW Japan situated along the continental margin before opening of Japan Sea (e.g., Otofuji et al 1985 a, b), because it has been suggested that the upper mantle beneath the continent has enriched geochemical character (e.g., Allegre et al., 1982; Hawkesworth et al 1983; Pearece , 1983).

Tectonic implication

Before the rotation of the SW Japan arc sliver, the volcanic rocks had relatively enriched Pb-Nd-Sr isotopic compositions. To explain the enriched isotopic compositions of HMAs relative to basalts, Ishizaka and Carlson (1983) advocated the existence of mantle keel as a enriched geochemical reservoir beneath the SW Japan arc. Likewise, Nohda and coworkers (1988) insisted on the existence of sub-continental lithosphere (SCL) as an enriched component beneath the NE Japan arc to explain enriched Nd-Sr isotopic compositions of volcanic rocks which had erupted before Japan Sea opening. Further, they suggested that the secular variation of Nd-Sr isotopic compositions had been induced by the thinning of SCL.

The stress field of SW Japan arc sliver is extensional during Japan Sea opening (e.g., Fourier and Jolivet, 1995; Northrup et al., 1995). Further, Tamaki (1995) had suggested that both Yamato and Tsushima basin are composed of thinned lower crust. Therefore, it seems to be suggested that the thinning of the enriched layer such as mantle keel mainly controlled the secular variations of Pb isotopic compositions. However, the depths of magma segregation of the both Osaka and Shodo-Shima HMAs, which had erupted pre- and post-rotation of SW Japan arc sliver, respectively, were inferred to be identical, those are 35 km (Tatsumi 1982). Further, the thickness of continental crust beneath the SW Japan is about 30-40 km (e.g., Yoshii et al., 1974). These would indicate that the magma segregations had occurred at the upper most mantle throughout the rotation of SW Japan arc sliver and that the depth of upper most mantle had been invariant during the rotation of SW Japan arc sliver. These would suggest that the thinning of lower crust or SCL would not have occurred at sub-Setouchi lower crust or upper mantle during the Setouchi volcanism. It is thus inferred that the thinning of SCL would not play an important role to characterize the isotopic compositions of Setouchi volcanic rocks. Further, based on the isotopic compositions of basalts and HMAs, it is suggested that the mantle keel also may not play a important role to characterize isotopic compositions of Setouchi volcanic rocks (see previous section).

The plausible mechanism to explain the geochemical secular variations would be replacement of the enriched mantle by depleted asthenospheric

materials. Following observations are consistent with this model. (1) The Nd-Sr isotopic compositions of Japan Sea BABB and the volcanic rocks from the back arc side of NE Japan exhibit secular variation (Nohda and Wasserburg, 1986; Nohda et al., 1988, 1992). (2) The Pb isotopic compositions of Japan Sea BABB form a single linear array, which is parallel with the trend of the Setouchi volcanic rocks (Tatsumoto and Nakamura, 1991; Cousens and Allan, 1992). (3) The chemical composition of Japan Sea BABB also show the compositional shift (Allan and Gorton, 1992). (4) the BABB source mantle material were chemically depleted (Yamashita and Tatsumi, 1994).

Taking the thickness of mantle wedge (less than 30 km) into the account, the depleted material should be the lateraly injected into sub-Setouchi mantle wedge. If this is the case, the following scenario is suggested for the origin of the Setouchi volcanic rocks. Positively/passively uprising asthenospheric materials which related to Japan Sea opening may cause replacement of the sub-Setouchi mantle wedge by the lateral asthenospheric mantle flow. The rotational movement of SW Japan sliver and the obduction over the newly born Philippine Sea plate might also be induced by this mantle flow. The direct introduction of hot asthenospheric materials and the obduction over hot lithosphere should attain extremely high temperature both in the mantle wedge and the subducted slab. This may caurse both the direct partial melting of the downgoing slab and the Setouchi volcanism (e.g., Drummond and Defant, 1990; Peacock et al., 1994; Tatsumi et al.,

1996). The geochemical secular variations of the Setouchi volcanic rocks would represent the replacement of the mantle wedge by injected asthenospheric materials. This asthenospheric injection is consistent with the steepening of subducted slab and trench retreatment which observed in NE Japan arc (Nohda et al., 1990; Tatsumi et al., 1990)

Although the Japan Sea opening had commenced at least 20 Ma (e.g., Kaneoka et al., 1990, 1992), the rotational movement of SW Japan sliver and the Setouchi volcanism suddenly occurred at 16 Ma and ceased at 14 Ma (e.g., Otofuji et al., 1985a,b, 1991; Ishikawa et al 1996), i.e., only active at the latest stage of Japan Sea opening. This might indicate that the arrival of hot asthenospheric materials induced both the rotational movement of SW Japan arc sliver and the Setouchi volcanism. This scenario may prefer the model that the Japan Sea opening caused by the positive asthenospheric uprising, and the relative motions, such as plate convergence rates, may not play an important role to precipitate Japan Sea opening (e.g., Northrup et al., 1995).

Conclusion

Sr, Nd and Pb isotopic compositions of basalts and HMAs from the Setouchi volcanic belt are systematically different, more enriched isotopic compositions for HMAs than basalts. This would be explained by processes in including that much larger amounts SDSCs are overprinted onto the magma source for HMA magmas than those for basalt magmas. Further, Pb isotopic compositions suggest that the major component of SDSC is derived from the subducted terrigenous sediment. However, in order to account for Pb concentrations of HMAs, the altered MORB crust derived component are also required.

Trace element characteristics of basalts and HMAs, especially systematically higher Zr/TiO_2 and Nb/TiO_2 ratios with lower TiO_2 concentrations of HMAs than those of basalts, would suggest that the metasomatic agent may be partial melt of the subducted slab and not hydrous fluids.

The secular variations of Pb isotopic compositions may suggest that the replacement of the sub-Setouchi mantle wedge by the depleted materials had occurred during the rotation of SW Japan arc sliver associates with the back arc opening. Possible materials with depleted geochemical signature would be the uprising deep-seated asthenospheric materials. The positively uprised asthenospheric materials, which had caused Japan Sea opening, would subsequently induce the rotational movement of the SW Japan sliver and the replacement of the sub Setouchi mantle wedge.

Acknowledgments

I wish to sincerely acknowledge Prof. S. Nohda in initiating Pb isotopic work in his laboratory of Kyoto Sangyo University, who has unselfishly shared much of his time and considerable knowledge. I also acknowledge for his critical comments and encouragement throughout this work.

I really appreciate Prof. B. M. Jahn of Univèrsite de Renne who kindly taught me the procedure of Pb isotopic analyses and the ethos of careful experimental science, without his great help this thesis should not have been completed.

I wish to thank Prof. Y. Tatsumi for his continued interest and passion in this work, and for many useful advices on many topics. His ability for simplicity of logic, clarity of thought and isolating the essence of most ponderous problems have made strong, and I hope lasting, impression upon me.

I am grateful to Prof. K. Ishizaka for leading me to such an interesting field and suggesting this work as possible thesis.

I am also thank Dr. N. Ishikawa, Dr. H. Shinjoe and Dr. T. Kogiso for their useful discussions. I wish to express my sincere thank to all above persons.

References

Allan, J. F., and M. P. Gorton, Geochemistry of the igneous rocks from Legs 127 and 128, Sea of Japan, Proceeding of the Ocean Drilling Program, Scientific Results,127/128, 905-929, 1992.

Allègre, C. J., B. Dupré, P. Richard, D. Rousseau, and C. Brooks, Subcontinental versus suboceanic mantle, II. Nd-Sr-Pb isotopic composition of continental tholriites with mid-ocean ridge tholeiites, and the structure of the continental lithosphere., Earth and Planetary Science Letters,57, 25-34, 1982.

Anno, K-Ar dating of the Setouchi volcanic rocks: Constraints on the timing and duration of rotation of the southwest Japan arc., master's thesis, Kyoto University, 1995.

Ben Othman, D., W. M. White, and J. Patchett, The geochemistry of marine sediments, island arc magma genesis, and crust-mantle recycling, Earth and Planetary Science Letters,94, 1-21, 1989.

Catanzaro, E. L., T. J. Murphy, W. R. Shields, and E. L. Garner, Absolute isotopic abundance ratios of common, equal-atom, and radiogenic lead isotopic standard., Jour. Res. Nation. Bereau Standard.,A, 72A, 261-267, 1968.

Cousens, B. L., and J. F. Allan, A Pb, Sr, and Nd isotopic study of basaltic rocks from the Sea of Japan, LEGS 127/128, Proceeding of the Ocean Drilling Program, Scientific Results,127/128, 805-836, 1992.

DePaolo, D. J., and G. J. Wasserburg, Inferences about magma sources and mantle stracture from variations of 143Nd/144Nd, Geophysical Research Letters,3, 743-746, 1976.

Douce, A. E. P., and D. Johnston, Phase equilibiria and melt productivety in the pelitic system: implications for the origine of peraluminous granitoids, Contribution to Mineralogy and Petrology,107, 202-218, 1990.

Douce, A. E. P., and J. S. Beard, Dehydration-melting of the biotite gneiss and quartz amphibolite from 3 to 5Kbar., Journal of Petrology,36, 707-738, 1995.

Drummond, M. S., and M. J. Defant, A model for torondhjemite-tonalite-dacite genesis and crustal growth via slab melting: archean to moderan comparisons., Journal of Geophysical Research,95, 21503-21521, 1990.

Ewart, A., The mineralology and petrology of Tertiary-Recent orogenic volcanic rocks: with special reference to the andesitic-basaltic compositional change., in vol. Andesite: orogenic andesites and related rocks., edited by Thrope, pp. 26-87, Wiley, 1982.

Fournier, M., and L. Jolivet, Neogene stress field in SW Japan and mechanism of deformation during the Sea of Japan opening., Journal of Geophysical Research,100, 24295-24314, 1995.

Furukawa, Y., and Y. Tatsumi, Partial melting of the subducted Philippine Sea plate beneth SW Japan at 15Ma: evidence from thermal modelling., in preparation,1996.

Gill, J. B. (1981). Orgenic andesites and plate tectonics. New York: Springer-Verlag.

Goto, A., and Y. Tatsumi, Quantitative analyses of rock samples by X-ray fluorescence spectrography (I), Rigaku-denki Journal (in Japanese),22, 28-44, 1991.

Goto, A., and Y. Tatsumi, Quantitative analyses of rock samples by X-ray fluorescence spectrography (II), Rigaku-denki Journal (in Japanese),23, 50-69, 1992.

Green, T. H., Anatexis of mafic crust and high pressure crystallization of andesite, in vol. Andesites, edited by R. S. Thrope, pp. John Wiley & Sons, 1982.

Hart, S. R., A large-scale isotope anomaly in the South Hemisphere mantle, Nature,309, 753-757, 1984.

Hawkesworth, C. J., A. J. Erlank, J. S. Marsh, M. A. Menzies, and P. van Calsteren, Evolution of the continental lithosphere: evidence from volcanics and xenoliths in southern Africa., in vol. Continental Basalt and Mantle Xenoliths, edited by C. J. Hawkesworth, and M. J. Norry, pp. 111-138, Shiva, Nantwich, 1983.

Hawkesworth, C. J., K. Gallagher, J. M. Hergt, and F. McDermott, Trace element fractionation processes in the generation of island arc basalts, Phil. Trans. R. Soc. of Lond.,342, 179-191, 1993.

Hayashida, A., Y. Otofuji, and M. Torii, Paleoposition of southwest Japan and convergence between Eurasia and Pacific plates in pre-Neogine time, Modern Geology,12, 467-480, 1988.

Hickey, R. L., F. A. Frey, and D. C. Gerlach, Multiple source for basaltic arc rocks from the southern volcanic zone of the Andes (34-41oS): trace element and isotopic evidence for contributions from subducted oceanic crust, mantle and continental crust., Journal of Geophysical Research,91, 5963-5983, 1986.

Ishikawa, T., and E. Nakamura, Origine of the slab component in arc lavas from across-arc variation of B and Pb isotope., Nature,370, 205-208, 1994.

Ishikawa, N., T. Anno, T. Itaya, and Y. Tatsumi, Rotation of the SW Japan arc sliver at 15 Ma: evidence from age and paleomagnetic tada for Setouchi volcanic belt, in preperation.,1996.

Ishizaka, k., and R. W. Carlson, Nd-Sr systematics of the Setouchi volcanic rocks, southwest Japan: a clue to the origine of orogenic andesite, Earth and Planetary Science Letters,64, 327-340, 1983.

Jolivet, L., and K. Tamaki, Neogene Kinematics in the Japan sea region and volcanic activety of the northeast Japan arc, Proceeding of the Ocean Drilling Program, Scientific Results,127/128, 1311-1327, 1992.

Kaneoka, I., K. Notsu, Y. Takigami, K. Fujioka, and H. Sakai, Constraints on the evolution of the Japan Sea based on 40Ar-39Ar ages and Sr isotopic ratios for volcanic rocks of Yamato seamount chain in the Japan Sea, Earth and Planetary Science Letters,97, 211-225, 1990.

Kaneoka, I., Y. Takigami, N. Takaoka, S. Yamashita, and K. Tamaki, 40Ar-39Ar analysis of volcanic rocks recovered from the Japan Sea Floor: Constraints on the age of formation the Japan Sea, Proceeding of the Ocean Drilling Program, Scientific Results,127/128, 819-836, 1992.

Karig, D. E., Origine and development of marginal basins in the western Pacific., Journal of Geophysical Research,76, 2542-2561, 1971.

Kelemen, P. B., N. Shimizu, and D. Todd, Relative depletion of niobium in some arc magmas and the continental: partitioning of K, Nb, La and Ce during melt/rock reaction in the uper mantle., Earth and Planetary Science Letters,120, 111-134, 1993.

Kersting, A. B., and R. J. Arculus, Pb isotope composition of Klyuchevskoy volcano, Kamchatka and North pacific sediments: Implications for magma genesis and crustal recycling in the Kamchatkan arc., Earth and Planetary Science Letters,136, 133-148, 1995.

Klein, D. G., Off-ridge volcanism and seafloor spreading in the Shikoku Basin., Nature,27, 746-748, 1978.

Klein, D. G., and K. Kobayashi, Geological summary of the north Philippine Sea, based on Deep Sea-Drilling Project Leg 58 results., Init. Rep. DSDP Leg 58,951-961, 1980.

Kobayashi, K., and M. Nakada, Magnetic anomalies and tectonic evolution of the Shikoku inter-arc basin., Journal of Physics of the Earth,26, 391-402, 1978.

McCulloch, M. T., and J. A. Gamble, Geochemical and geodynamical constraints on subduction zone magmatism., Earth and Planetary Science Letters,102, 358-374, 1991.

Morris, J. D., W. P. Leeman, and F. Tera, The subducted component in island arc lavas: constraints from Be isotopes and B-Be systematics., Nature,344, 31-36, 1990.

Navon, O., and E. Stolper, Geochemical consequences of melt percolation: The upper mantle as a chromatographic column., Journal of Geology,95, 285-307, 1987.

Nicholls, I. A., and A. E. Ringwood, Effect of water on olivine stability in tholeiites and production of silica-saturated magmas in the island arc environment., Journal of Geology,81, 285-300, 1973.

Nohda, S., and G. J. Wasserburg, Trends of Sr and Nd isotopes through time near the Japan Sea in the northeastern Japan., Earth and Planetary Science Letters,78, 157-167, 1986.

Nohda, S., Y. Tatsumi, Y. Otofuji, T. Matsuda, and K. Ishizaka, Asthenospheric injectionand back-arc opening: isotopic evidence from northeast Japan., Chemical Geology,68, 317-327, 1988.

Nohda, S., Y. Tatsumi, S. Yamashita, and F. Toshitsugu, Nd and Sr isotopic study of Leg 127 basalts: implications for the evolution of the Japan Sea backarc basin, Proceeding of the Ocean Drilling Program, Scientific Results,127/128, 899-904, 1992.

Northrup, C. J., L. H. Royden, and B. C. Burchfield, Motion of the Pacific plate relative to Eurasia and its potential relation to Cenozoic extension along the eastern margine of Eurasia., Geology,23, 719-722, 1995.

Otofuji, Y., and T. Matsuda, Paleomagnetic evidence for the clockwise

rotation of southwest Japan., Earth and Planetary Science Letters,62, 349-359, 1983.

Otofuji, Y., and T. Matsuda, Timing of rotational motion of southwest Japan inferred from paleomagnetism., Earth and Planetary Science Letters,85, 289-301, 1984.

Otofuji, Y., T. Matsuda, and S. Nohda, Paleomagnetic eviidences for the Miocene countereclockwise rotation pf northeast Japan-Rifting process of the Japan arc, Earth and Planetary Science Letters,75, 265-277, 1985.

Otofuji, Y., T. Itaya, and T. Matsuda, Rapid rotation of southwest Japan-Paleomagnetism and K-Ar ages of MIocene volcanic rocks of southwest Japan, Geophysical Journal of International,1991.

Peacock, Fluid proceses in subduction zone, Science,248, 329-337, 1990.

Peacock, S. M., T. Rushmer, and A. B. Thompson, Partial melting of subducting oceanic crust, Earth and Planetary Science Letters,121, 227-244, 1994.

Pearce, J. A., Role of the sub-continental lithosphere in magma genesis at active continental margine., in vol. Continental Basalt and Mantle Xenoliths, edited by C. J. Hawkesworth, and M. J. Norry, pp. 230-249, Shiva, Nantwich, 1983.

Pearce, J. A., and D. W. Peate, Tectonic implications of the composition of volcanic arc magmas., Annual Review of Earth and Planetary Sciences,23, 251-285, 1995.

Poli, S. M., and M. W. Schmidt, Water tarnsprot and release in subduction zone: experimental constraints on basaltic and andesitic systems., Journal of Geophysical Research,100, 22299-22314, 1995.

Richard, R., N. Shimizu, and C. J. All`gre, 143Nd/144Nd, a natural tracer: an application to oceanic basalts., Earth and Planetary Science Letters,31, 269-278, 1976.

Ringwood, The petrological evolution of island arc systems, Journal of Geological Society of London,130, 183-204, 1974.

Saito, M., Y. Bando, and H. Noda, Fossil molluscous from Teshima, Shodogun, Kagawaprefecture, southwest Japan., Trans. Proc. Paleontol. Soc. Japan,77, 276-289, 1970.

Sakuyama, M., and I. Kushiri, Vesiculation of hydrous andesitic melt and transport of alkalis by separated vapor phase., Contribution to Mineralogy and Petrology,71, 61-66, 1979.

Sato, H., Geology of Goshikidai and adjacent areas, northeast Shikoku, Japan : Field occurrence and petrography of sanukitoid and associated volcanic rocks., Sci. Rep. Kanazawa Univ.,27, 13-70, 1982.

Shaw, H. R., Trace element fractionation during anatexis., Geochimica Cosmochimica et Acta,34, 237-243, 1970.

Stolper, E., and S. Newman, The role of water in the petrogenesis of Mariana trough magmas., Earth and Planetary Science Letters,121, 293-325, 1994.

Sun, S. s.-. , Lead isotopic study of young volcanic rocks from mid-ocean ridges, oceab islands and island arcs, Phil. Trans R. Soc. Lond.,A297, 409-445, 1980.

Sun, S.-s., and W. F. McDonough, Chemical and isotopic systematics of oceanic basalt: implecations for mantle composition and processes, in vol. 42, Magmatism in Ocean Bains, edited by A. D. Saubders, and M. J. Norry, pp. 313-345, Geological Society Special Publication, 1989.

Taira, A., and N. Niitsuma, Turbidite sedimentation in the Nankai trough as interpreted from magnetic fabrics, grain size, and detrital model analyses, Initial Report of the Deep Sea Drilling Project.,LXXXVII, 611-632, 1985.

Tamaki, K., Opening tectonics of the Japan Sea, in vol. Backarc Basin: Tectonics and Magmatism, edited by B. Taylor, pp. 407-420, Plenum Press, New York, 1995.

Tatsumi, Y., and K. Ishizaka, Existence of andesitic primary magma: an example from southwest Japan., Earth and Planetary Science Letters,54, 124-130, 1981.

Tatsumi, Y., Melting experiment on a high-magnesian andesite, Earth and Planetary Science Letters,54, 357-365, 1981.

Tatsumi, Y., Origine of high-magnesian andesites in the Setouchi volcanic belt, southwest Japan, II. Melting phase relations at high pressures, Earth and Planetary Science Letters,60, 305-317, 1982.

Tatsumi, Y., and K. Ishizaka, Origine of high-magnesian andesites in the Setouchi volcanic belt, sputhwest Japan, I. Petrographical and chemical

characteristics., Earth and Planetary Science Letters,60, 293-304, 1982.

Tatsumi, Y., and K. Ishizaka, High-magnesian andesite and basalt from the Shodo-Shima Island, southwest Japan, and theirbearingon the genesis of calc-alkaline andesite., Lithos,15, 161-172, 1982.

Tatsumi, Y., Volcanic geology of Shodo-shima island, Kagawa prefecture, sowthwest Japan, and its bearing on paleoenvironment of Seto Inland Sea area., Journal of Geological Society of Japan,89, 693-706, 1983.

Tatsumi, Y., D. L. Hamilton, and R. W. Nebitt, Chemical characteristics of fluid phase released from a subdeuted lithosphere and origine of arc magmas: evidence from high pressure experiments and natulal rocks., Jurnal of Volcanology and Geothermal Reserch,29, 293-309, 1986.

Tatsumi, Y., S. Nohda, and K. Ishizaka, Secular variation of magma source compositions beneath the northeast Japan arc, Chemical Geology,68, 309-316, 1988.

Tatsumi, Y., and S. Maruyama, Boninites and high-Mg andesites: tectonics and petrogenesis, in vol. Boninites, edited by A. J. Crawford, pp. 50-71, Unwin Hyman, London, 1989.

Tatsumi, Y., S. Maruyama, and S. Nohda, Mechanism of backarc opening in the Japan Sea: role of asthenospheric injection., Tectonophysics,299-306, 1990.

Tatsumi, Y., M. Murasaki, E. M. Arsadi, and S. Nohda, Geochemistry of Quaternary lavas from NE Sulawesi: transfer of subduction components into the mantle wedge., Contribution to Mineralogy and Petrology,107, 137-149, 1991.

Tatsumi, Y., M. Murasaki, and S. Nohda, Across-arc variation of lava chemistry in the Izu-Bonin arc: identification of sabduction component., Journal of Volcanology and Geothemal Research,49, 179-190, 1992.

Tatsumi, Y., Y. Furukawa, and S. Yamashita, Thermal and geochemical evolution of the mantle wedge in the northeast Japan arc: 1. Contribution from experimental petorology, Journal of Geophysical Research,99, 22275-22283, 1994.

Tatsumi, Y., Y. Furukawa, N. Ishhikawa, G. Shimoda, M. Torii, and H. Shinjoe, Melting of slab and production of high-Mg andesite magmas: unusual magmatism in SW Japan at 13-15 Ma, in preperation,1996.

Tatsumoto, M., and Y. Nakamura, DUPAL anomaly in the sea of Japan: Pb, Nd, and Sr isotopic variations at the eastern Eurasian continental margine, Geochimica Cosmochimica et Acta,55, 3697-3708, 1991.

Taylor, B., and G. D. Karner, On the evolution of marginal basins, Review of Geophysics and Space Physics,21, 1727-1741, 1983.

Terra, F., I. Brown, J. Morris, I. S. Sacks, J. Klein, and R. Middleton, Sediment incorporation in island-arc magmas: inferences from 10Be., Geochimica Cosmochimica et Acta,50, 535-550, 1986.

Toksöz, M. N., and A. T. Hsui, Numerical Studies of back-arc convection and the formation of marginal basins, Tectonophysics,50, 177-196, 1978.

Torii, Paleomagnetism of Miocenerocks in Setouchi province: evidence for rapid clockwise rotation of southwet Japan at midle Miocene time, Doctor, Kyoto, 1983.

Vielzeuf, D., and J. R. Holloway, Experimental determination of the fluid-absent melting relations in the pelitic system.
Consequences for crustal differetiation, Contribution to Mineralogy and Petrology,98, 257-276, 1988.

Wasserburg, D. J., S. B. Jacobsen, D. J. DePaolo, M. T. McCluloch, and T. Wen, Precise determination of Sm/Nd ratios, Sm and Nd isotopic abundances in standard solutions., Geochimica Cosmochimica et Acta,45, 2311-2323, 1981.

White, W. H., and B. Dupr`e, Sediment subduction and magma genesis in the Lesser Antilles: isotopic and trace element constraints., Journal of Geophysical Research,91, 5927-5941, 1986.

Willie, P. J., and T. Sekine, The formation of mantle phlogopite in subduction zone hybridization., Contribution to Mineralogy and Petrology,79, 375-380, 1982.

Yamashita, S., and Y. Tatsumi, Thermal and geochemical evolution of the mantle wedge in the northeast Japan arc 2. Contribution from geochemistry., Journal of Geophysical Research,99, 22285-22293, 1994.

Yoshii, T., Y. sasaki, T. Tada, H. Okada, S. Asano, I. Muramatu, M. Hashizume, and T. Moriya, The third Kurayoshi explosion and the crustal structure in the western part of Japan, Journal of Physics of the Earth,22, 109-121, 1974.

Yuhara, M., Timing of intrusion of the Otagiri granite with respect to the deformation and metamorphism in Ryoke belt in the Ina district, central Japan: Examination by the Rb-Sr whole rock isochron ages., Gankou,89, 269-284, 1994.

Appendix 1

Lead Isotope Analyses : An Application to GSJ Standard Rock Samples

Abstract

Experimental procedures of Pb isotopic analyses on rock samples are described. Bromide form anion exchange chromatography technique was adopted to separate Pb from acid-decomposed sample. Extreme care was exercised to minimize Pb contamination throughout the analytical procedures. Pb contamination was low enough and precise Pb isotopic compositions of rock samples were determined. Silica-gel activator method was employed to obtain enhanced emission of Pb ions in the mass spectrometer. Repeated analyses of SRM 981 standard were performed with various sample size and filament current, which enabled to determine suitable conditions for Pb isotopic analysis. Based on these results, mass fractionation factor to correct mass fractionation was obtained. We applied this procedure to GSJ (Geological Survey of Japan) standard rock samples. The results agree with reported data for these standard rocks, suggesting that the present procedures are reliable in determining Pb isotopic compositions of rock samples.

1. Introduction

Pb isotopic compositions are important geochemical tracers for the study of crust-mantle differentiation and many petrogenetic problems (e.g. Zindler & Hart, 1986). In addition, Pb isotopic compositions can be used to assess environmental pollution (e.g. Graney et al., 1995). Precise analyses of Pb isotope composition, however, often encounter two analytical difficulties. One is Pb contamination during sample processing, because Pb is ubiquitously contained in urban air. The other is in the correction for mass fractionation, since there is no internal stable isotope ratio for Pb. Consequently, interlaboratory comparison of Pb isotopic data may not always be possible.

To overcome these difficulties, two breakthroughs were established during the 1960s. Development of ion exchange chromatography method using anion exchange resin in Br-form reduced the total elution volume and separation time, because distribution coefficients for Br form anion exchange resin between Pb and the other elements are largely different. Silica-gel activator method developed by Akinshin et al. (1957) and Cameron et al. (1969) enhanced the emission of Pb ions and prevented mass fractionation effect.

I apply these methods with minor modification for precise determination of Pb isotopic composition. To overcome the problem of mass fractionation effect, external standard samples such as Standard Reference Materials (SRM) of U.S. National Bureau of Standards (NBS),

especially SRM 981 for which the absolute isotopic compositions of Pb are known, was determined with our method. By analyzing SRM 981, it is also possible to compare the results from different laboratories. I further determined the suitable condition for Pb isotope analyses by changing both sample size of SRM 981 and filament current.

In this appendix, I report the analytical procedure of Pb isotope compositions and the scheme for correcting mass fractionation effect. In addition, I present Pb isotopic compositions of the GSJ standard rock samples.

2. Experiment

2-1. Chemical procedures

Reagents

H_2O is passed through mix bed resin, then distilled using a pyrex® apparatus, further purified with a Milli-Q® purifier, and finally sub-boiled by using quartz apparatus. All chemical procedures were performed using this pure water. HBr, HF, and HNO_3 (WAKO PURE CHEMICAL INDUSTRIES Ltd., special grade, 47%, 46% and 61%, respectively) were distilled with a two-bottle teflon still, twice, four times, three times, respectively. HCl (WAKO PURE CHEMICAL INDUSTRIES, Ltd., special grade, 35%) was diluted to 6.2 N, and then distilled with a quartz apparatus, and finally distilled (sub-boiled) twice with a two-bottle teflon still. H_3PO_4 (MERCK, ultra pure grade) was diluted to 0.1 N, then passed through two cycles of cation exchange resin column (Bio-Rad AG50W-X12®) and anion exchange

resin column (Bio-Rad AG-1X8®). $HClO_4$, purchased from NBS, was directly used in our experiment. Silica powder was washed several times by pure nitric acid and were preserved in pure water.

Decomposition

About 100 mg of a powdered standard rock sample was placed in a PFA® teflon vial with a screw cap and decomposed with 1 ml of hydrofluoric (about 20 N) acid and 1 ml of nitric acid (about 14 N) with a few drops of perchloric acid (about 10 N). The bottom half of the sample vial was immersed in ultrasonic bath for ten to thirty minutes to promote decomposition, and heated in an electric oven set at constant temperature (90 °C) for three to seven days for complete decomposition.

The completely decomposed sample was dried in the small hand-made "clean box" which is a kind of closed system consisting of an acrylic box with a HEPA® filter. By using this system, I can minimize the environmental contamination during drying samples. The completely dried sample was dissolved in the 1 ml of 6 N HCl, then dried and converted to chloride form.

Chemical separation

The procedure of chemical separation of Pb from the decomposed samples is summarized in Fig. 1. Lead is the only element that is retained

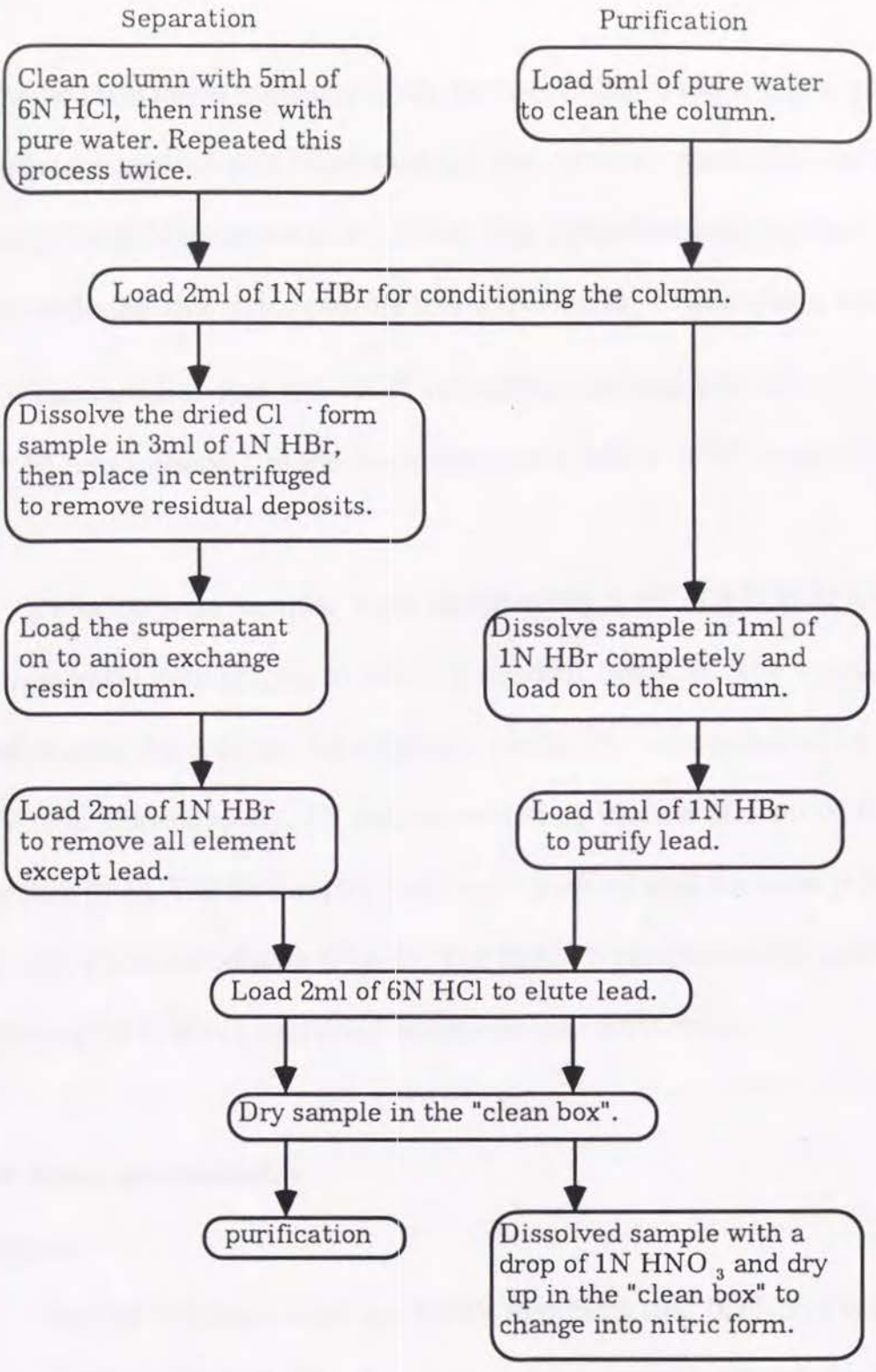

Fig. 1. The experimental scherne for separation and purification pf Pb from acid-decomposed samples.

in the Br form anion exchange resin, because Pb has a much higher partition coefficient against that resin than all the other elements (Korkisch and Hazan, 1965, Matsumoto et al., 1986). The separation and purification was done utilizing this principle. In this experiment, I used anion exchange resin column (Bio-Rad AG-1X8® 100-200 mesh) that is 3 mm in diameter and 30 mm in height, made from shrinkable teflon TFE® tube (NORTON Inc.).

Chloride form samples were dissolved by 3 ml of 1 N HBr and were subsequently centrifuged to remove residual deposits. The solution was loaded on to the column. All elements, except Pb, were removed by 2 ml of 1 N HBr. Subsequently, Pb was recovered by elution of 2 ml of 6 N HCl and then dried. The Pb samples were again purified with the same procedures through the same column (Fig. 1). The final Pb samples were dissolved by a drop of 14 N HNO_3 and dried to convert into nitric form.

2-2. Mass spectrometry

Filament

The Re filaments used are 0.025 mm thick and 0.75 mm wide. The purity of Re is 99.97%. The filaments were outgassed at 4.0 A for 30 to 60 minutes. The thermal ionization was carried out by the use of single filament mode.

Sample loading

Dried Pb sample was completely dissolved by 4 ml silica-gel and 3 ml of 0.01 N phosphoric acid. 0.5 ml of the dissolved sample was loaded carefully onto a small area at the center of the filament. The filament current was then increased slowly up to about 1.0 A in order to dry the sample. This process was repeated until all sample solution was loaded and dried. Subsequently, the filament current was slowly increased to about 2.2 A, until the filament becomes dark-red, then kept dark-red for about 2 seconds. All sample loading procedure were performed using binocular microscope under laminar flow of filtered air.

Mass spectrometry

Finnigan MAT 260 thermal ionization mass spectrometer operated by HP9133 computer at Kyoto Sangyo University was used for Pb isotopic analyses. The accelerating voltage was adjusted to 10 kV. Collector system is a single Faraday cup with a resistance of $10^{11}\ \Omega$. The data acquisitions were made by peak switching between 204 amu, 206 amu, 207 amu, 208 amu for mass peaks, and 204.5 amu for baseline. The raw data were processed for base line correction and bilinear correction by on-line system.

3. Results and Discussions

Blanks

The total procedure blanks are usually much higher than the sum of the amount of impurity in reagents (e.g. Koide and Nakamura, 1989). Since

the measured total procedure blanks in our laboratory were 62 pg, they are expected to be about 50-100 pg. This suggests that the influence of blanks to the isotopic composition of Pb is negligible, if sample size of Pb is more than 10 ng.

Suitable condition for isotope analyses and the determination of mass fractionation factor

When I analyze Pb isotopic composition, I must make corrections for the mass fractionation effect which occurs in the mass spectrometer. In the case of Pb, there is no stable isotope ratio, therefore I cannot correct mass fractionation by the method applied to other isotope systems such as Nd and Sr. To overcome this problem, I must use an external standard. In the present study, I adopted NBS SRM 981 as the standard and Pb isotopic compositions were repeatedly determined for various sample sizes (2000 ng, 1000 ng, 500 ng, 200 ng, 100 ng, 50 ng, 25 ng), and ion beam intensities (below 1 V, 1-2 V, above 2 V).

From the present results, the following conditions should be maintained to obtain coherent isotopic composition. (1) Pb sample on the filament should be controlled between 100-1000 ng. (2) Mass analysis should be done in the range of ion beam intensity between 1-2 V. The reasons for this are given below.

In the case where the amount of Pb is larger than 1000 ng, coherent and high precision data with good reproducibility is attained for ion beam

intensities above 2 V (Fig. 2). However, mass fractionation effect will be enhanced at higher ion beam intensities, and the obtained values must be evaluated with caution. Therefore it is recommended that the sample size be kept below 1000 ng and intensities below 2 V. On the other hand, if the amount of Pb is less than 50 ng, mass fractionation effect is much advanced during analysis (Fig. 2), hence I should not analyze Pb isotopic composition when the amount of Pb is less than 50 ng. Finally, if the amount of Pb is higher than 100 ng and less than 1000 ng, the ion beam intensity should not be raised above 2 V, since this possibly leads to advanced mass fractionation. In the case where ion beam intensity is below 1 V, I cannot obtain accurate data regardless of sample size.

To confirm the reproducibility and precision, I analyzed NBS SRM 981 under the suitable condition repeatedly. As shown in Fig. 3 and 4, analytical data under the suitable condition are tightly grouped around the mean values, suggesting that the mass fractionation effect is not advanced. The mean Pb isotopic compositions and their standard deviation (1 σ) of 17 analyses are $^{206}Pb/^{204}Pb = 16.900 \pm 0.005$, $^{207}Pb/^{204}Pb = 15.440 \pm 0.007$ and $^{208}Pb/^{204}Pb = 36.529 \pm 0.020$. From now on, I will refer to this suitable condition as the "reliable condition".

I also show data obtained under different conditions (Fig. 3) in which the mean Pb isotopic compositions and their standard deviation (1 σ) of 27 analyses were $^{206}Pb/^{204}Pb = 16.917 \pm 0.028$, $^{207}Pb/^{204}Pb = 15.463 \pm 0.031$ and $^{208}Pb/^{204}Pb = 36.621 \pm 0.089$. These values are markedly higher than

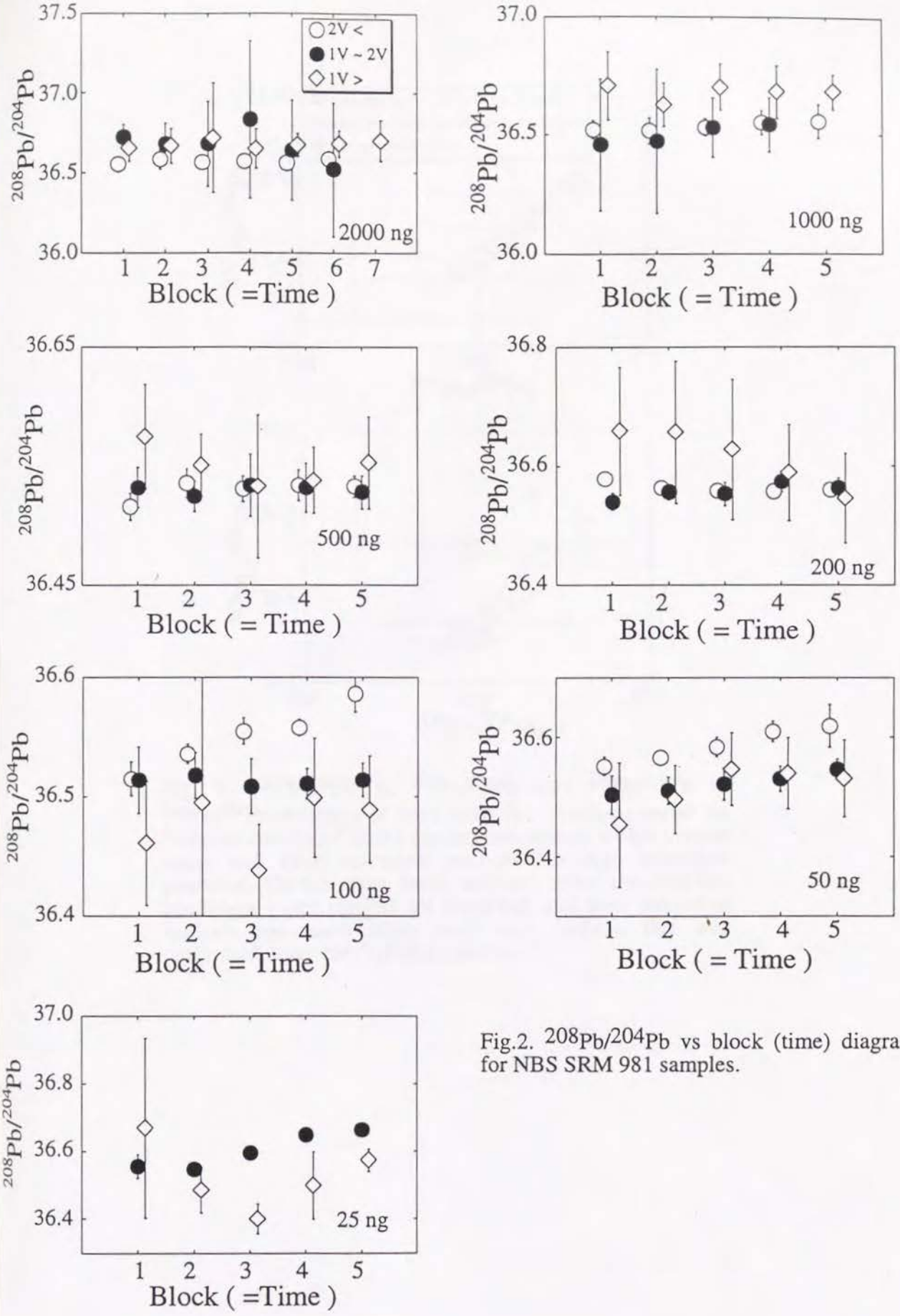

Fig.2. $^{208}Pb/^{204}Pb$ vs block (time) diagrams for NBS SRM 981 samples.

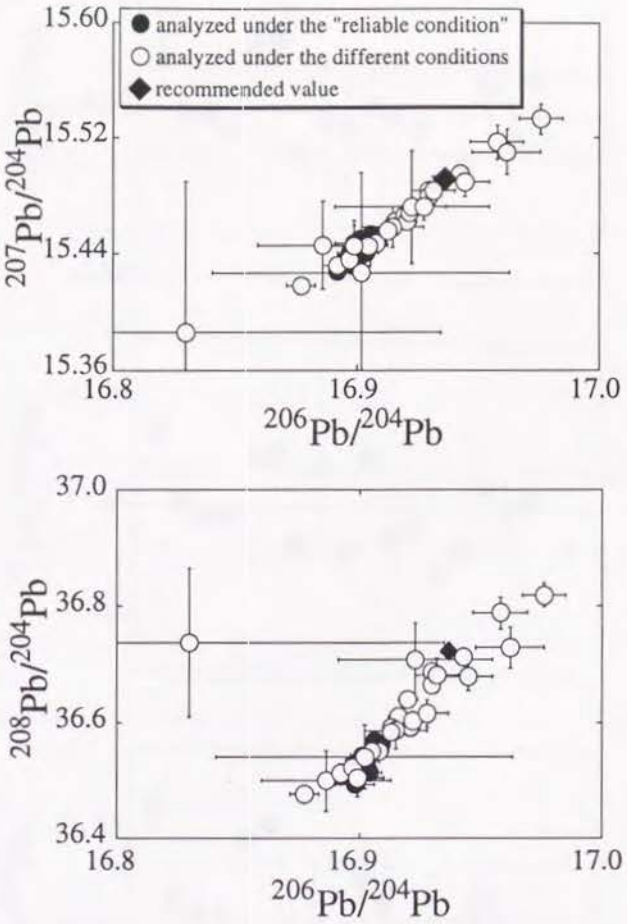

Fig. 3. $^{206}Pb/^{204}Pb$ vs $^{207}Pb/^{204}Pb$ and $^{206}Pb/^{204}Pb$ vs $^{208}Pb/^{204}Pb$ diagrams of NBS SRM 981. Analyses under the "reliable condition" (solid circles) concentrate within narrow range and their individual analysis has high analytical precision. On the other hand, analyses under the different conditions (open circles) are dispersed, and their individual analysis has much larger error than analysis that was performed under the "reliable condition".

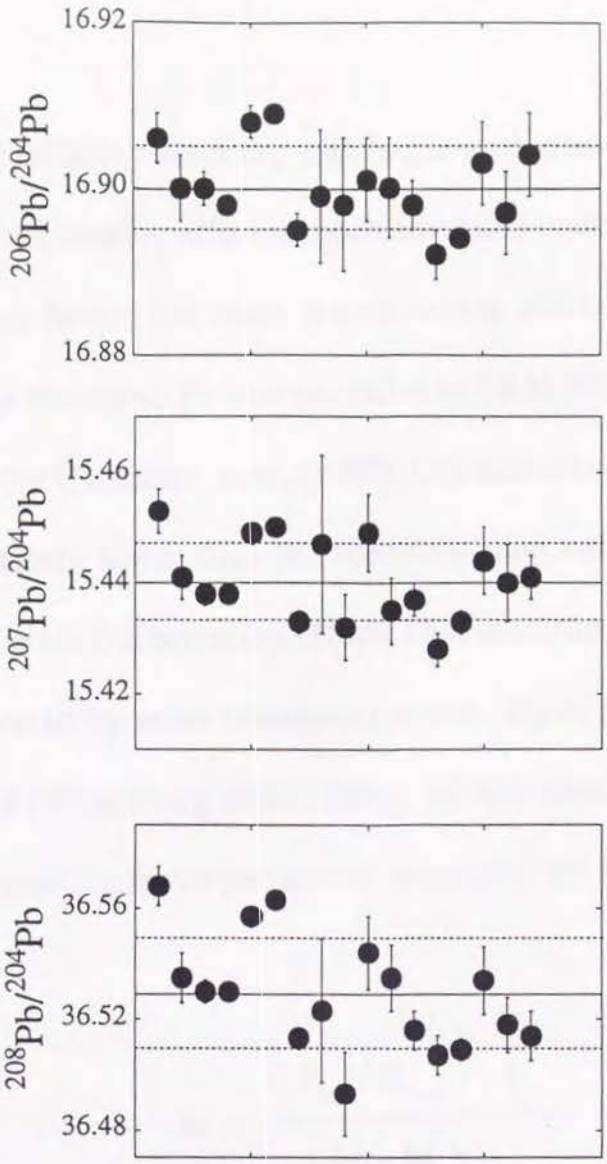

Fig. 4. Variations of individual analysis of $^{206}Pb/^{204}Pb$, $^{207}Pb/^{204}Pb$, $^{208}Pb/^{204}Pb$ and their errors. Each error bar indicate 2 sigma mean. The solid lines indicate the mean value of 17 separate analyses of NBS SRM 981, and the broken lines indicate their standard deviations

those under the reliable condition, with larger analytical errors. This indicates that the mass fractionation effect is much advanced under different conditions.

Correction factor for mass fractionation effect was determined by normalizing the measured Pb isotopic ratios of SRM 981 to the recommended value obtained by Catanzero et al., (1968). Our data show good reproducibility but were definitely lower than the recommended values (Fig. 3) which is caused by the mass fractionation effect. This systematic shift of Pb isotopic ratio is interpreted by mass fractionation law. Three fractionation laws are generally used (Wasseburg et al., 1981). In this experiment, I adopted the linear law. Correction factor per atomic mass unit "α" is calculated following equation.

$$\alpha = \frac{(R_{ref} / R_{meas}) - 1}{(M_i - M_j)}$$

Rref and Rmeas are isotope ratios of two isotopes i and j, whose masses are M_i and M_j, respectively. The reference isotope ratios (Catanzero et al., 1963) are $^{206}Pb/^{204}Pb = 16.937$, $^{207}Pb/^{204}Pb = 15.491$ and $^{208}Pb/^{204}Pb = 36.721$.

Using the above values and equation, I obtain the mass correction factor "α". In our laboratory, the mass fractionation factors for $^{206}Pb/^{204}Pb$, $^{207}Pb/^{204}Pb$ and $^{208}Pb/^{204}Pb$ are 0.11 %/amu, 0.11 %/amu and 0.13 %/amu, respectively. Calculated correction factor for $^{208}Pb/^{204}Pb$ is obviously different, therefore I use two correction factors. I compared the

correction factors from different laboratories (Table 1). This indicates that mass fractionation effect during analysis in our laboratory is within an acceptable range.

Analytical precision and accuracy

The standard deviations (1 σ) of 17 analyses for $^{206}Pb/^{204}Pb$, $^{207}Pb/^{204}Pb$ and $^{208}Pb/^{204}Pb$ analyzed under the reliable condition, are ± 0.005, ± 0.007 and ± 0.020, which correspond to 0.03%, 0.05% and 0.05%, respectively. On the other hand, those which were analyzed under "different conditions" (27 analyses) are ± 0.028, ± 0.031 and ± 0.089, which correspond to 0.16%, 0.20% and 0.24%. This indicates that the data analyzed under the different conditions were widely scattered. In contrast, data analyzed under the reliable condition have good reproducibility. This probably due to the variable degree of mass fractionation effect, mainly much advanced mass fractionation effect, under the "different" conditions. Also, in the view of accuracy, I should analyze Pb isotopic composition under the reliable condition. It should be noted that the accuracy of Pb isotopic composition can not attain the same level as precision.

Application to GSJ standard rock samples

I analyzed Pb isotopic compositions of GSJ standard rock samples under the reliable condition to confirm the reliability of our analyses (Table 2).

Table 1. Correction factors from different laboratoies

Correction Factor	References
0.14%/amu	White et al., G.C.A., 49, (1985), 1875-1886
0.10%/amu	Woodhead &Fraser, G.C.A., 49, (1985), 1925-1930
0.08%/amu	Graham et al., G.C.A., 56, (1985), 2797-2819
0.15%/amu	Tastumoto & Nakamura, G.C.A., 55, (1991), 3697-3708
0.10%/amu	McDermott et al., Contrib. Mineral. Petrol., 113, (1993), 9-23
0.13%/amu	Koide & Nakamura, Mass Spectoroscopy, (1989)
0.09%/amu for $^{206}Pb/^{204}Pb$ and $^{207}Pb/^{204}Pb$ 0.13%/amu for $^{208}Pb/^{204}Pb$	Mukasa et al., E.P.S.L., 84, (1987), 153-164
0.10%/amu for $^{206}Pb/^{204}Pb$ and $^{207}Pb/^{204}Pb$ 0.13%/amu for $^{208}Pb/^{204}Pb$	Barreiro, G.C.A., 47, (1983), 817-822
0.11%/amu for $^{206}Pb/^{204}Pb$ and $^{207}Pb/^{204}Pb$ 0.13%/amu for $^{208}Pb/^{204}Pb$	This work

Table 2 Pb isotopic compositions of GSJ of standard rock samples

	This work			Reference data*		
Rocks	$^{206}Pb/^{204}Pb$	$^{207}Pb/^{204}Pb$	$^{208}Pb/^{204}Pb$	$^{206}Pb/^{204}Pb$	$^{207}Pb/^{204}Pb$	$^{208}Pb/^{204}Pb$
JA-1	18.289 +/- 0.002**	15.522 +/- 0.001	38.228 +/- 0.004	18.295 +/- 0.018***	15.530 +/- 0.015	38.231 +/- 0.039
				18.308 +/- 0.058	15.548 +/- 0.041	38.265 +/- 0.115
				18.307 +/- 0.037	15.535 +/- 0.033	38.239 +/- 0.082
JA-2	18.403 +/- 0.005	15.599 +/- 0.003	38.655 +/- 0.010	18.425 +/- 0.050	15.637 +/- 0.039	38.757 +/- 0.106
				18.411 +/- 0.101	15.644 +/- 0.039	38.777 +/- 0.268
JB-1	18.327 +/- 0.003	15.549 +/- 0.003	38.615 +/- 0.008			
JB-2	18.332 +/- 0.003	15.555 +/- 0.003	38.223 +/- 0.006	18.335 +/- 0.059	15.548 +/- 0.055	38.215 +/- 0.142
				18.328 +/- 0.042	15.547 +/- 0.045	38.259 +/- 0.102
JG-1	18.631 +/- 0.009	15.667 +/- 0.010	38.901 +/- 0.023	18.561 +/- 0.070	15.570 +/- 0.070	38.531 +/- 0.174
	18.630 +/- 0.007	15.643 +/- 0.006	38.849 +/- 0.011	18.532 +/- 0.062	15.586 +/- 0.061	38.584 +/- 0.138
	18.595 +/- 0.002	15.614 +/- 0.002	38.763 +/- 0.005			

* Koide and Nakamura (1989)
** Errors are 2 sigma mean
*** Errors are standard deviation

Lead isotopic compositions of GSJ standard rock samples.

The errors given in our analyses are 2 sigma-mean (or 2 standard errors), whereas those reported by Koide and Nakamura (1989) were in one standard deviation. Therefore, I cannot make direct comparison between the analytical precisions of the two laboratories. However, our results are in good agreement with their data within the range of their analytical errors. But for JG-1, even though the difference is within their analytical error, our data are slightly different from their data. It is difficult to determine whether this was caused by difference in experimental procedures, especially the correction of mass fractionation effect, or by heterogeneity of standard rock sample. The latter is considered more plausible, because isotopic composition of other standard rock samples show good agreement.

4. Conclusions

1. Using Br form anion exchange resin I have effectively separated and purified Pb from rock samples for Pb isotopic analyses.

2. Application of the silica-gel activator method with limited sample sizes (100 ng to 1000 ng) and limited ion beam intensities (1 V to 2 V) enables to obtain Pb isotopic compositions with high precision and good reproducibility.

3. Pb blanks through all procedures were 50-100 pg, which was insignificant for isotope ratio correction for Pb sample size more than 10 ng.

4. Good reproducibility is demonstrated by 17 analyses of NBS SRM 981 standard. The uncertainties (in 1 σ) for $^{206}Pb/^{204}Pb$, $^{207}Pb/^{204}Pb$ and $^{208}Pb/^{204}Pb$ are 0.03 %, 0.05 % and 0.05 %, respectively.

5. Upward correction factors per amu for $^{206}Pb/^{204}Pb$, $^{207}Pb/^{204}Pb$ and $^{208}Pb/^{204}Pb$ ratios are 0.11 %, 0.11 % and 0.13 %, respectively.

6. Analyses of GSJ standard rock samples indicate that our procedure is reliable in determination of Pb isotopic compositions of rock samples.

Acknowledgments

We thank Professor Bor-ming Jahn of Universite de Rennes, France, for many precious advice and suggestions during the course of this study. Indeed, without his help, this work would not have been possible. We are much indebted to Professor Kyoichi Ishizaka of Graduate School of Human and Environmental Studies of Kyoto University and Professor Yoshiyuki Tatsumi of Integrated Human Studies of Kyoto University for encouraging discussions. We thank Ms. R. Arai for reviewing the early draft.

REFERENCES

Akisin, P.A., Nikitin, O.T. & Panchenkov, O.T. Geokhimiya 5, 429 (1957).

Barreiro, B. Geochimica et Cosmochimica Acta 47, 817-822 (1983).

Cameron, A.E., Smith, D.H. & Walker, R.L. Analitical Chemistry 41, 525 (1969).

Catanzaro, E.L., Muurphy, T.J., Shields, W.R. & Garner, E.L. Journal of Research. U. S. National Bureau of Standard, Section A 72A, 261 (1968).

Graham, I.J., Gulson, B.L., Hedenquist, J.W. & Mizon, K. Geochimica et Cosmochimica Acta 56, 2797-2819 (1992).

Graney, J.R., Halliday, A.N., Keeler, G.J., Nariagu, J.O., Robbins, J.A., & Norton, S.A. Geochimica et Cosmochimica Acta 59, 1715-1728 (1995).

Koide, Y. & Nakamura, E. Mass Spectroscopy (1989).

Korkisch, J. & Hazan, I. Analitical Chemistry 37, 707 (1965).

Matumoto, A., et al. Bunseki Kagaku 35, 590 (1986).

McDermotte, F., Defant, M.J., Hawkesworth, C.J., Maury, R.C. & Joron, J.L. Contribution to Mineralogy and Petrology 113, 9-23 (1993).

Mukasa, S.b., McCabe, R. & Gill, J.B. Earth and Planetary Science Letters 84, 153-164 (1987).

Tastumoto, M. & Nakamura, Y. Geochimica et Cosmochimica Acta 55, 3697-3708 (1991).

Wasserburg, G.J., Jacobsen, S.B., DePaolo, M.T. & McCulloch, M.Y. Geochimica et Cosmochimica Acta 45, 2311 (1981).

White, W.M., Dupr, B. & Vidal, P. Geochimica et Cosmochimica Acta 49,

1875-1886 (1985).

Woodhead, J.D. & Fraser, D.G. Geochimica et Cosmochimica Acta 49, 1925-1930 (1985).

Zindler, A. & Hart, S. R. Annual Reviews Earth Planet Science 14, 493-570 (1986).